From Anonymous Referee #1

The MS titled "Atmosphere–ocean exchange of heavy metals and polycyclic aromatic hydrocarbons in the Russian Arctic Ocean" written by Ji et al. researched the results of a Russian Arctic assessment of the occurrences and atmosphere–ocean fluxes of 35 polycyclic aromatic hydrocarbons (PAHs) and 9 metals (Pb, Cd, Cu, Zn, Fe, Mn, Ni, and Hg). The topic of this study is quite interesting due to the reflection of anthropogenic influences in the normal biochemical cycles as the balance of geochemical substances between ocean and gas. Authors pointed out the net input of Hg and 35 PAHs into ocean, filling the data gaps in this field. The deposition including dry and wet deposition in the Arctic Ocean so far appeared very sporadic data without a continuous sampling sites and period. The topic of this MS is within scope of ACP, the language usage and structure of article is generally good and well-written. However, there are still some minor problems and some questions remained. I would like to support this MS to be published unless my questions and problems are well addressed or answered. There are specific questions I found in this MS.
Response: thank you very much for your valuable and helpful comments and suggestions on our manuscript.

1. L43-44, it's quite not logic here, authors should introduce the transported pollutants from low attitude to the polar region as the Arctic rather than the present statements about reducing global emissions. Additionally, global emissions of the atmospheric pollutants were carried by monsoon to the high latitude. What is the contribution of it to the Arctic area? Are there any reports concerning the separate contribution of airborne pollutants to land and ocean?
Response: initially, we tried to show Arctic air pollution includes harmful trace gases (e.g. tropospheric ozone) and particles (e.g. black carbon, sulphate) and toxic substances (e.g. polycyclic aromatic hydrocarbons) that can be transported to the Arctic from emission sources located far outside the region, or emitted within the Arctic from activities including shipping, power production, and other industrial activities **(Arnold et al. 2015)**. We realized it's not appropriate to put global emissions here with a specific contribution to the Arctic. We will put more references about Arctic air pollutants' transport for better illustration here.

Arnold, S.R., Law, K.S., Brock, C.A., Thomas, J.L., Starkweather, S.M., Salzen, K. von ., Stohl, A., Sharma, S., Lund, M.T., Flanner, M.G., Petäjä, T., Tanimoto, H., Gamble, J., Dibb, J.E., Melamed, M., Johnson, N., Fidel, M., Tynkkynen, V.-P., Baklanov, A., Eckhardt, S., Monks, S.A., Browse, J. and Bozem, H., 2016. Arctic air pollution: Challenges and opportunities for the next decade. Elem Sci Anth, 4, p.000104. DOI: http://doi.org/10.12952/journal.elementa.000104

2. L46, the reason mercury is key problematic pollutant should be briefly mentioned here. And citation is needed here.
Response: we have revised this sentence as "mercury is a key problematic pollutant in the Arctic because mercury is a neurotoxic pollutant seriously influencing northern latitudes through human exposure originated from eating seafood and marine mammals as traditional diets by hunting and fishing (Stow et al., 2015)" in **line 46-48, Page 3**.

L47, what kind of sources are referring here?

Response: the sources could be as the resulting sea ice loss may increase accessibility of the Arctic, leading to increases in air pollutant emissions within the Arctic from activities such as oil and gas extraction or shipping. It is thought that Northern Hemisphere mid-latitude emissions (from Europe, Asia, and North America) are currently the main source of air pollutants in the Arctic (**Stohl, 2006; Sharma et al., 2013**), including also toxic contaminants with important atmospheric pathways (e.g. mercury (Hg), certain persistent organic pollutants (POPs). However, sources of air pollution from within the Arctic or nearby sub-Arctic (defined here as 'local') are already important in some regions **(Stohl et al. 2013)**, and these and other sources may grow rapidly in the future **(Corbett et al., 2010; Peters et al., 2011)**. We will revise this part of information.

Shindell D, Faluvegi G. 2009. Climate response to regional radiative forcing during the twentieth century. Nat Geosci 4: 294–300. doi: 10.1038/ngeo473.

Stohl A. 2006. Characteristics of atmospheric transport into the Arctic troposphere. J Geophys Res 111: D11306. doi: 10.1029/2005JD006888.

Sharma S , Ishizawa M , Chan D , Lavoue D , Andrews E , et al. 2013. 16-Year simulation of Arctic black carbon: Transport, source contribution, and sensitivity analysis on deposition. J Geophys Res 118: D017774. doi: 10.1029/2012JD017774.

Stohl A , Klimont Z , Eckhardt S , Kupiainen K , Shevchenko VP , et al. 2013. Black carbon in the Arctic: The underestimated role of gas flaring and residential combustion emissions. Atmos Chem Phys 13: 8833–8855. doi: 10.5194/acp-13-8833-2013.

Peters G , Nilssen T , Lindholt L , Eide M , Glomsrød S , et al. 2011. Future emissions from shipping and petroleum activities in the Arctic. Atmos Chem Phys 11: 5305–5320. doi: 10.5194/acp-11-5305-2011.

Corbett JJ , Lack DA , Winebrake JJ , Harder S , Silberman JA , et al. 2010. Arctic shipping emissions inventories and future scenarios. Atmos Chem Phys 10: 9689–9704. doi: 10.5194/acp-10-9689-2010.

3. L49, "the melting of contaminated ice" in the ocean or also in the terrestrial land?

Response: In here, we meant both melting ice in ocean as well as the melting snow in the terrestrial soils since fluxes from thermokarst rivers would bring the pollutants into the ocean as another source.

4. L68, what is relevant connection between benthic input of metals and air-seawater exchange input?

Response: It has been reported that a large fraction of the organic matter that forms in surface waters in the shelf areas of the Chukchi Sea sinks to the sea floor, which fuels productive

benthic communities and causes high rates of sedimentary denitrification **(Chang and Devol, 2009; Brownetal., 2015)**. The Pacific origin water from the Bering Strait is already deplete dinitrate relative to phosphate, and NO_3^- is further depleted relative to PO_4^{3-} in the Chukchi Sea via the effect of sedimentary denitrification **(Yamamoto-Kawaietal.,2006)**. A unique feature of the upper surface water in the western Arctic Ocean is the dominance of a strong, cold halocline that separates the Pacific-origin surface waters from the underlying Atlantic-origin waters **(Aagaardetal.,1981)**. And metals in deep ocean showed the similar pattern of nutrients (**Brownetal., 2015)**.

Chang, B.X., Devol,A.H., 2009. Seasonal and spatial patterns of sedimentary denitrification rates in the Chukchi sea. Deep Sea Res. II56(17), 1339–1350.

Yamamoto-Kawai, M., Carmack, E., McLaughlin, F., 2006. Nitrogen balance and Arctic through flow. Nature 443,43.

Aagaard, K., Coachman,L.K.,Carmack,E., 1981.On the halocline of the Arctic Ocean. Deep Sea Res. 28A(6), 529–545.

Brown,Z.W., Casciotti,K.L., Pickart,R.S., Swift,J.H., Arrigo,K.R., 2015.Aspects of the marine nitrogen cycle of the Chukchi Sea shelf and Canada Basin. Deep Sea Res. II 118,73–87.

5. L88-89, the sentence authors make here tried to indicate the inorganic salt ions may increase during the summer melting season, and thence the organic compounds' solubility would change? Now the meaning is not clear. Authors need to rephase the sentences to clarify.
Response: we will make this sentence clear. We intended to state that inorganic salts are appreciably soluble in organic media, principally of the oxygenated forms (alcohols, ketones, ethers, esters), when they are capable of forming neutral molecules in solution. This property is largely confined to the transition elements. Those of the first long series, and in the trans-radium region, accomplish this without forming undebatably covalent compounds; other subgroup elements which are solvent-soluble show a stronger tendency toward covalent bond formation, and may show solubility in chlorinated hydrocarbons and benzenoid solvents in which the first group mentioned are not usually soluble. The salts of the first three groups of the periodic table generally are not organic-soluble, because their co-ordinative power is relatively low, and their solid lattice energies are high.

6. L91, need citation for "the Arctic Ocean is considered as a sink that receives global airborne pollutants".
Response: we have added a reference for the source of this sentence in **line 87, Page 4**.

7. L203, how surface chlorophyll concentrations were calculated or measured?
Response: Spectrophotometry method was used to measure chlorophyll concentrations. It involves the collection of a fairly large water sample, filtration of the sample to concentrate the chlorophyll-containing organisms, mechanical rupturing of the collected cells, and

extraction of the chlorophyll from the disrupted cells into the organic solvent acetone. The extract is then analyzed by either a spectrophotometric method (absorbance or fluorescence), using the known optical properties of chlorophyll, or by HPLC. This general method, detailed in Section 10200 H. of Standard Methods, has been shown to be accurate in multiple tests and applications and is the procedure generally accepted for reporting in scientific literature.

8. L218, why H' can be corrected by the salinity? In Fick's law, I am not aware of such connection. H' values are usually considered by the temperature changes.
Response: usually temperature an salinity can be both used to correct Harry laws. However, the salinity of seawater has been indirectly determined by means of electrical conductivity. Since the absolute conductivity cannot be measured as accurately as required for precise salinity measurements **(Seitz et al., 2010)**, the conductivity has been measured relative to that of standard seawater; the conversion to salinity is carried out by means of the (relative) conductivity–salinity relation PSS-78 **(JPOTS, 1981a, b)**. In practice, this is achieved by calibrating salinometers and conductivity–temperature–depth devices using standard seawater, which is diluted to obtain the conductivity of the potassium chloride standard **(Culkin, 1986; Bacon et al., 2007)** used as a conductivity reference. An unconditional prerequisite for the comparability of salinity measurements over long periods is, therefore, that the salt proportions in standard seawater are stable. Unfortunately, this cannot be guaranteed, as standard seawater is of natural origin.

Seitz, S., Spitzer, P., and Brown, R. J. C.: CCQM-P111 study on traceable determination of practical salinity and mass fraction of major seawater components, Accredit. Qual. Assur., 15, 9–17, https://doi.org/10.1007/s00769-009-0578-8, 2010.

Joint Panel on Oceanographic Tables and Standards (JPOTS): Tenth report of the Joint Panel on Oceanographic Tables and Standards – The Practical Salinity Scale 1978 and The International Equation of State of Seawater 1980, Unesco technical papers in marine science, 36, 13–17, UNESCO, Paris, France, available at: http://unesdoc.unesco.org/images/0004/000461/046148eb.pdf , 1981a.

Joint Panel on Oceanographic Tables and Standards (JPOTS): Background papers and supporting data on the Practical Salinity Scale 1978, Unesco technical papers in marine science, 37, UNESCO, Paris, France, available at: http://unesdoc.unesco.org/images/0004/000479/047932eb.pdf , 1981b.

Bacon, S., Culkin, F., Higgs, N., and Ridout, P.: IAPSO standard seawater: definition of the uncertainty in the calibration procedure and stability of recent batches, J. Atmos. Ocean. Tech., 24, 1785–1799, https://doi.org/10.1175/JTECH2081.1, 2007.

Culkin, F.: Calibration of standard seawater in electrical conductivity, Sci. Total Environ., 49, 1–7, https://doi.org/10.1016/0048-9697(86)90230-5, 1986.

9. L246, how the uncertainty of air-water exchange net direction was conducted?

Response: we will add this information to the supplementary information. We take the method from Liu et al. (2016).

Liu, Y., Wang, S., McDonough, C. A., Khairy, M., Muir, D., and Lohmann, R.: Estimation of Uncertainty in Air–Water Exchange Flux and Gross Volatilization Loss of PCBs: A Case Study Based on Passive Sampling in the Lower Great Lakes, Environmental Science & Technology, 50, 10894-10902, 10.1021/acs.est.6b02891, 2016.

To evaluate the uncertainty in air-water fugacity ratio and the statistically calculated diffusive flux, measured uncertainties of water and air analysis, Henry's law constant, temperature and overall velocity of mass transfer were taken into account. Four variables with random uncertainty of the fugacity ratio was based on Eq. (11) and Eq. (13), of which the uncertainty is shown in Eq. (S1).

$$\delta \ln\left(\frac{f_g}{f_w}\right) = \sqrt{\left(\frac{\delta C_g}{C_g}\right)^2 + \left(\frac{\delta C_w}{C_w}\right)^2 + \left(\frac{\delta H'}{H'}\right)^2 + \left(\frac{\delta T}{T}\right)^2} \quad \text{(S1)}$$

The relative standard deviation (RSD) of aqueous and water concentrations ($\left(\frac{\delta C_g}{C_g}\right)$ and $\left(\frac{\delta C_w}{C_w}\right)$) are relevant to the analysis. The RSDs of H' was taken value as 50%.

10. L263, why only OH radicals were considered to the degradation of PAHs in the atmosphere?

Response: Dry deposition is more effective than wet deposition as a removal process from the atmosphere. Chemical reactions provide the other main sink for atmospheric PAHs. The gas phase reactions of PAHs with the OH radical, the NO_3 radical and ozone have been widely investigated. Available rate coefficient data are most abundant in the case of the OH radical. The established mechanism of PAH reactions with the OH radical involves the formation of a PAH–OH adduct followed by further reaction with NO_2 or O_3. The observed reaction products include both ring-retaining nitro-PAHs and quinones, as well as ring-opened products such as phthalic acid, phthalaldehyde and phthalic anhydride. The presence of methyl groups in methyl naphthalenes and methyl phenanthrenes in most cases leads to a modest increase in reactivity relative to the parent PAH. For NO3 reactions, the predominant reaction pathway involves NO3 addition followed by reaction with NO_2 leading to nitro-PAH formation. The observed rate coefficients are proportional to the nitrogen dioxide concentration. There have been far fewer studies of the gas phase reactions of PAH with ozone.

11. L279-280, Do author have any proofs to support the reason with air trajectories of Russian Arctic?

Response: this reason with air trajectories of Russian Arctic was observed by the previous study **(Shevchenko et al. 2003)**.

V. Shevchenko, A. Lisitzin, A. Vinogradova, R. Stein. Heavy metals in aerosols over the seas of the Russian Arctic. The Science of the Total Environment 306 (2003) 11–25.

12. L294, which sea Taymyr Peninsula is closer to? Clarify here. L295, I think Shevchenko et al. 2013 should be moved to previous sentence.
Response: this phase has been revised as "On the Taymyr Peninsula (adjacent to Kara Sea and Leptev Sea)" in **line 301 Page 11**. The sentence of Shevchenko et al. 2013 has been moved to previous sentence.

L419, Can authors explain what molecular weight PAHs were easier to de degraded in the air because it's important for biocycles to consume these carbon sources by organisms. If most of heavy molecular PAHs enter ocean ecosystem, which may not be consumed by biota.
Response: theoretically, lighter PAHs can be easier degraded. Photo-induced toxicity of PAHs can be driven from formation of intracellular singlet oxygen and other reactive oxygen species (ROS) that cause oxidative damage in biological systems **(El-Alawi et al., 2002)**, or formation of photo-products, which exert different, often stronger, bioactivity than the parent compound **(Grote et al., 2005)**.

Measurement of short- and long-term toxicity of polycyclic aromatic hydrocarbons using luminescent bacteria. El-Alawi YS, McConkey BJ, George Dixon D, Greenberg BM Ecotoxicol Environ Saf. 2002 Jan; 51(1):12-21.

Modeling photoinduced algal toxicity of polycyclic aromatic hydrocarbons. Grote M, Schüürmann G, Altenburger R Environ Sci Technol. 2005 Jun 1; 39(11):4141-9.

L440, I suggest authors to put some information of future protective measures for this region.
Response: according to your suggestion, we have added the future protective measures for this region in the end of conclusion part.

From Anonymous Referee #2

Review of "Atmosphere-ocean Exchange of heavy metals and polycyclic aromatic hydrocarbon in the Russian Arctic Ocean".

This work reports the concentrations of PAHs and metals in air, water and snow in the Russian sector of the Arctic. There is no previous data for this sector, so this contribution is very important. The work is of mix quality, with sections that are generally well done, but other material that is erroneous or needs further work. The manuscript needs some work in order to present the data appropriately, improve the comparison with other studies for polar regions, and give some extra depth to the discussion. This revision is mainly for the PAHs part. I suggest moderate to major modifications before it can be accepted.
Response: we are very grateful that you spent your valuable time reviewing our manuscript and giving us good comments and suggestions to help us revise this manuscript!

1. Line 40. Comment and cite a work on long-range atmospheric transport of PAHs (or pops) to the arctic.
Response: according to the reviewer's suggestion, a citation about 20 years monitoring POPs in the Arctic (**Hung et al. 2016**), has been added in **Line 39 Page 3**.

Hung, H., Katsoyiannis, A. A., Brorström-Lundén, E., Olafsdottir, K., Aas, W., Breivik, K., Bohlin-Nizzetto, P., Sigurdsson, A., Hakola, H., Bossi, R., Skov, H., Sverko, E., Barresi, E., Fellin, P., and Wilson, S.: Temporal trends of Persistent Organic Pollutants (POPs) in arctic air: 20 years of monitoring under the Arctic Monitoring and Assessment Programme (AMAP), Environ. Pollut., 217, 52-61, https://doi.org/10.1016/j.envpol.2016.01.079, 2016.

2. Line 49-50. Provide examples, there are some published for Antarctica and the Arctic for both metals and pahs.
Response: we have carefully searched Web of Science. Some relevant references concerning PAHs and heavy metals in air deposition and sea in the Arctic that we have added as examples in **Line 49-57 Page 3**.

3. Note that not all PAHs are persistent, it also depends if they are found in the gas or dissolved phase (less persistent) or associated to aerosols and particulate matter.
Response: thank you for pointing out this important note. In the examples we added, we have clarified that aerosols contained PAHs deposited into sea ice and soils (or snow) which is an important source for the contribution of persistent PAHs. Indeed, according to the previous study (**Fernandes and Sicre, 1999**), the major PAHs either from adjacent areas or low latitudes are in the form of aerosols and binding with black carbon (particulate matter).

Fernandes, M. B., and Sicre, M. A.: Polycyclic Aromatic Hydrocarbons in the Arctic: Ob and Yenisei Estuaries and Kara Sea Shelf, Estuarine, Coastal and Shelf Science, 48, 725-737, https://doi.org/10.1006/ecss.1999.0472, 1999.

4. Line 73. Biogeochemical instead of biochemical
Response: "biochemical" has been changed to "biogeochemical" in **Line 80 Page 4**.

5. Line 77-79. Specify if you are referring to rain or snow, or both. I guess snow.
Response: we have specified the wet deposition as snow deposition in **Line 87 Page 4**.

6. Line 110. This citation is not adequate here.
Response: we realized the methods here concerning simultaneous sampling both for gas and aerosol phase PAHs. The citations of details about these two methods have added in Line

7. Line 116. I guess that first in aluminum foil and after in polyethylene bags, which must be air-tight.
Response: after air sampling in the ship, we did kept the samples in folded aluminium foil firstly. This sentence has been revised as "the filters and PUFs were firstly covered with aluminum foil tightly for air-tightness, then immediately placed in polyethylene bags and zip the bags, and frozen at -20 °C prior to chemical analyses." in **Line 122-123 Page 6**.

8. Line 119. Was snow melted immediately? How was snow melted?
Response: no, snowfall samples were not melted immediately. After sampling, all samples were protected from light and stored at 4 °C in borosilicate glass bottles prior to the analysis. Snowfall samples were melted thoroughly at room temperature. This information has been added in **Line 130 Page 6**.

9. Line 123. M3 or L, these are huge volumes. I have never seen such large volumes for water using a XAD. Unless there is a typo mistake, such volumes need a justification and discussion.
Response: Thank you for pointing out this mistake. The unit should be "mL". This mistake has been corrected in **Line 130 Page 6**. We only used XAD-2 resin rather than XAD-4 resin for high volume of water. Water was filtered at a flow rate averaging 4 L/min with a pneumatic pump (Flojet) through a borosilicate microfiber glass filters (1 mm nominal pore size), housed in an aluminum filter support.

10. Line 265. It cannot be equation 13.
Response: we are sorry for this mistake. The hydroxyl radicals concentrations [OH] in the considered mixed layer (between 1,000 and 500 hPa) was based on the zonally and monthly averaged concentrations of OH radicals from **Spivakovsky and coworkers (2000)**. Therefore, this sentence has been removed.

Spivakovsky, C. M. et al. Three-dimensional climatological distribution of tropospheric OH: update and evaluation. J. Geophys. Res. 105, 8931-8980 (2000).

11. Line 266. Is this concentration appropriate for the arctic? Discuss.
Response: This is a very good question to discuss! We must admit that there is no ranges or exact data of OH radical levels in troposphere of polar regions.

Firstly, the primary source of HO radical in the troposphere is the photolysis of O_3 to produce O (^1D). This reaction requires radiation of wavelength less than 315nm, otherwise (O^3P) is produced. The latter species reacts with molecular oxygen in the presence of N_2 or O_2 to produce O_3. The electronically excited O(^1D) usually relaxes to produce (O^3P) but also undergoes reaction with water to produce HO. While minor sources of HO are available through reaction of O(^1D) with CH_4 and N_2. Therefore, the methods to measure OH concentrations were usually based on observed distributions of O_3, H_2O, NO_t (NO_2+NO+$2N_2O_5$+NO_3 +HNO_2+HNO_4), CO, hydrocarbons, temperature, and cloud optical depth.

Thus, it is difficult to compare the OH concentrations by different methods and altitudes as well as latitudes. **Hewitt and Harrison (1985)** summarized the OH concentrations in different altitude as well as the global mean, which showed the range of 0.5-5 × 10^6 mol cm^{-3} for daytime OH radical. **Li et al. (2008)** used an empirical method is presented to determine effective OH concentrations in the troposphere and lower stratosphere, based on CH_4, CH_3Cl, and SF_6 data from aircraft measurements (IAGOS-CARIBIC) and a ground-based station (NOAA). The results showed tropospheric OH average values of 10.9 × 10^5 (σ = 9.6 × 105) mol cm^{-3} in a global level. The reason we used data from **Spivakovsky and coworkers (2000)** is that the estimation of OH concentrations considered by latitudes ($\pm 32^o$) in Northern Hemisphere.

It should be noted that precipitation amounts in the Arctic are very low (annual precipitation on Svalbard is 150-300 mm). This means that wet scavenging is not efficient and the lifetime for soluble species like aerosols is longer than on the continents to the south. Gas- phase chemical removal of trace compounds all but stops in the Arctic atmosphere during the polar night. In the absence of sunshine, the production rate of the OH radical, which is the main gas-phase scavenger, is low. Also, in the sunlit part of the year, the chemical lifetime of trace compounds is relatively long in the polar atmosphere (except in the near-surface layer that is impacted by snowpack photochemical processes), due to the strong attenuation of short wave visible sunlight as the solar elevation is low and the low specific humidity. Therefore, the OH radicals in the Arctic troposphere should be further measured throughout the year. So far, OH radicals levels are within the global levels.

C.N. Hewitt, Roy M. Harrison, Tropospheric concentrations of the hydroxyl radical—a review,
Atmospheric Environment (1967), Volume 19, Issue 4, 1985, Pages 545-554.

Li, Mengze; Karu, Einar; Brenninkmeijer, Carl; Fischer, Horst; Lelieveld, Jos; Williams, Jonathan; 2018; npj Climate and Atmospheric Science, (1): 29.

Spivakovsky, C. M. et al. Three-dimensional climatological distribution of tropospheric OH: update and evaluation. J. Geophys. Res. 105, 8931-8980 (2000).

12. Line 269-270. I cannot understand this sentence if these estimations have just been explained.

Response: the uncertainty (error propagation) analysis basically used the relative standard deviation (RSD) based on measured uncertainties in air and water analysis, air−water partitioning coefficients (including Henry's law constant and temperature), and overall mass transfer velocity were considered. The equation we have added in **Text S1 Supplementary Materials**.

13. Line 370. In addition to the highest, provide the range for each basin. Generally, the values commented here do not correspond always to the values seen in Figure 5.

Response: the range of $\sum_{35}$ PAH concentrations in gas, aerosols and dissolve water for each basin has been added in **Line 373-397 Page 14-15**. We have checked the original data in Figure 5, some wrong concentration values have been revised in this paragraph (**Line 379-395, Page 14**).

14. Line 372. The concentrations in aerosols are extremely high! These need a comparison with other studies and a discussion. Which is the black carbon concentration in aerosol for this region?

Response: we are very sorry that this concentration was showing wrong in the paper. It cannot be so high. All concentrations should be divided 100. We have made corrections for graphs and texts. There are some reports concerning PAH concentrations in atmosphere in Ocean. However, not all separating gas and particle phase. Therefore, we only compared and discussed with the separated ones as "$\sum_{35}$ PAH concentrations in aerosols (C_A, ng m^{-3}) in the Barents Sea (0.25-2.95), and East Siberian Sea (0.24-3.32) with average C_A values of 1.38 and 2.07 ng m^{-3} respectively were apparently higher than those in the Leptev Sea (0.23-0.89) and Kara Sea (0.23-0.27) with average CA values of 0.30 and 0.25 ng m^{-3}, respectively (Fig. 5b). The average CA of $\sum_{35}$ PAH in present study is higher than those of $\sum_{64}$ PAH measured in South Atlantic Ocean (mean = 0.93 ng m^{-3}) and North Pacific Ocean (mean = 0.56 ng m-3) while much lower than those of $\sum_{64}$ PAH in Indian Ocean (mean = 10 ng m-3) (Gonzalez-Gaya et al., 2016). Considering average $\sum_{35}$ PAH C_A (1.02 ng m^{-3}) in the Russian Arctic Ocean, the value is comparable to those of $\sum_{64}$ PAH observed in South Atlantic Ocean and South Pacific Ocean (both mean = 1.1 ng m^{-3}) (Gonzalez-Gaya et al., 2016). The levels of $\sum_{18}$ PAH C_A were measured from North Pacific towards the Arctic Ocean with the range from 0.0002 to 0.36 ng m^{-3}, with the highest concentration found in the coastal areas in East Asia (Ma et al., 2013). These concentrations were significantly lower than the averages levels found in our study. Besides, Ma et al. (2013) observed the relatively higher $\sum_{18}$ PAH C_A in the most northern latitudes of the Arctic Ocean, which is associated with back trajectories of air masses from Sothern Asia. The higher levels of C_A in our study could be attributed to the costal line close to larger burning taiga forest and more industrial sources in the boreal regions of Russian continent. Similar to the pattern for heavy metals mentioned above, high levels of these chemicals may have been derived from atmospheric transport from the industrial areas of the Russian continent. Because different sampling methods, different measured total PAH species and not all reports separated gas and particles concentrations, it is quite difficult to compare PAH levels in the aerosols." In **Line 376-394 Page 14**.

As for black carbon concentration in aerosol, we did not establish the filter-based techniques or direct techniques to measure them in our study. From other studies (**Figures**), we could see that Concentrations are low in the Arctic compared with lower latitudes and come mostly from outside the area and there are lots of black carbon emission which can be transported to the Arctic regions. We think the connections between black carbon and PAHs contents can be further studied.

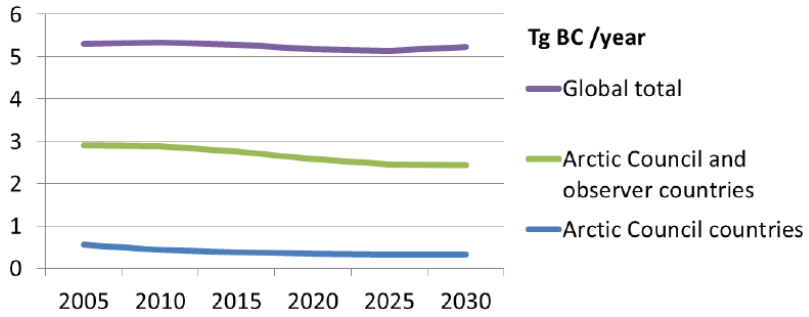

Sources: MACEB project (www.maceb.fi), IIASA-GAINS model.

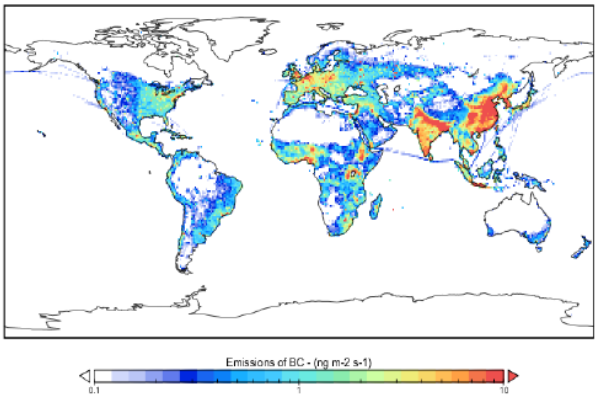

Source: UNEP/WMO 2011. United Nations Environment Programme , World Meteorological Organization (WMO), Integrated Assessment of Black Carbon and Tropospheric Ozone. 2011. http://2011_integrated-assessment-SUMMARY_UNEP-WMO.pdf

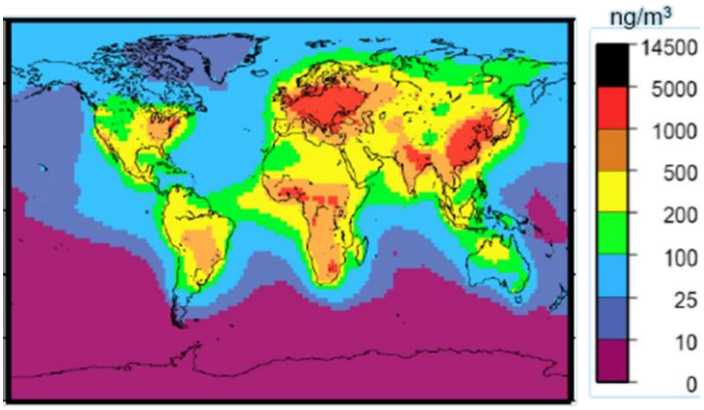

Source: Koch, D et al. Corrigendum to "Evaluation of black carbon estimations in global aerosol models" published in Atmos. Chem. Phys., 9, 9001-9026, 2009, Atmos. Chem. Phys., 10, 79–81, https://doi.org/10.5194/acp-10-79-2010, 2010.

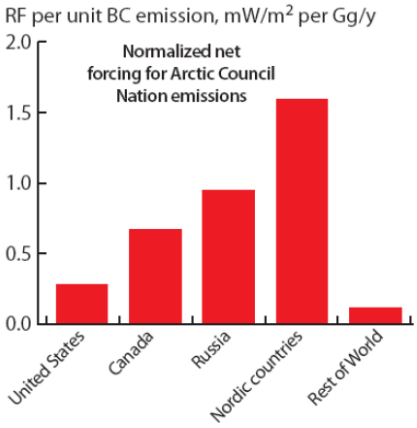

Source: AMAP, 2011. The Impact of Black Carbon on Arctic Climate (2011). By: P.K. Quinn, A. Stohl, A. Arneth,T. Berntsen, J. F. Burkhart, J. Christensen, M. Flanner, K. Kupiainen, H. Lihavainen, M. Shepherd, V. Shevchenko,H. Skov, and V. Vestreng. https://www.amap.no/documents/download/977/inline

15. Generally, compare the pahs and metal concentrations with other reports for the Arctic, even if these are for the north atlantic and north pacific.

Response: we have added the comparison both for metals and PAHs in the manuscript (**Page 11, 14-15**). However, we only compared with the similar sampling methods. Some of them with other method as unit “ng/g” for air concentrations were incomparable with our study. therefore, we didn’t compare these publications.

16. Line 391. Here or in the methods, comment the range of estimated dry deposition velocities.

Response: the range of dry deposition velocities (V_d) is important to calculate the dry deposition fluxes. V_d for each individual PAH may vary significantly. We have added the discussion as "The increasing values of dry deposition (V_d) may influence F_{DD} in the marine environment due to the higher hydrophobicity of organic compounds, surface microlayer with reduced surface tension, and lipid floating (del Vento and Dachs, 2007b). The apparently higher average V_d was observed for 9-methlyfluorene (1.01-10.02 cm s^{-1}) followed by 1,7-dimethylfluorene (1.06-10.63 cm s^{-1}) (**Fig. S6**). In the global scale, higher V_d was found for heavier PAHs such as methylchrysene (0.17-13.30 cm s^{-1}) and dibenzo(a,h)anthracene (0.29-1.38 cm s^{-1}) and other heavier PAHs (Gonzalez-Gaya et al., 2014). The V_d values reported previously ranged from 0.08 to 0.3 cm s^{-1} in the Atlantic Ocean (Del Vento and Dachs, 2007a), from 0.01 to 0.8 cm s^{-1} coastal areas (Holsen and Noll, 1992;Bozlaker et al., 2008;Esen et al., 2008;Eng et al., 2014). The previous reports showed a higher V_d values in concentrated industrial and urban areas (Bozlaker et al., 2008). In our study, the highest V_d values were observed in Barents Sea and the other three seas did not show the statistical differences ($p > 0.05$) except for 9-methlyfluorene and 1,7-dimethylfluorene. East Siberian Sea showed the lowest value of V_d while the relatively higher Vd values were found for heavier PAHs (dibenzo(a,h)anthracene, indeno(1,2,3-cd)pyrene, dibenzo(a,h)anthracene and benzo(g,h,i)perylene) in all the seas (**Fig. S7**). This may be explained by heavier PAHs are principally deposited via heavier aerosols with a quicker V_d because of bound with hydrophobic aerosols or gravity such as soot carbon having a faster V_d (Gonzalez-Gaya et al., 2014)." in **Line 309-427 Page 15**.

17. Line 395. Huge values, If possible compare with other measures. Report as well the concentrations in snow.

Response: we have recalculated our data and revised the values and unit. In the most references, the measurement for wet depositions was similar with use of high-volume air sampler for snow and rain, and the sample media consisted of a glass fiber filter (GFF) to trap airborne particles, followed by a self-packed PUF/XAD-2 glass column. As for papers focusing on new methods of measuring wet deposition we did not consider to compare in our paper. We have added some comparisons with other regions, however, some reference with too low wet deposition such as snowpack from lakes of Western U.S. National Parks (0.005 μg m^{-2} y^{-1} to 0.1μg m^{-2} y^{-1}) (**Usenko et al. 2010**) were not considered due to too limited sources compared to our study.

Usenko, S.; Simonich, S. L. M.; Hageman, K. J.; Schrlau, J. E.; Geiser, L.; Campbell, D. H.; Appleby, P. G.; Landers, D. H. Sources and Deposition of Polycyclic Aromatic Hydrocarbons to Western U.S. National Parks. Environ. Sci. Technol. 2010, 44 (12), 4512– 4518, DOI: 10.1021/es903844n

We have added the content as "The wet deposition flux of the ∑35 PAHs (F_{WD}, μg m-2 d-1) ranged from 14 to 19. Gonzalez-Gaya et al. (2014) found the highest F_{WD} of ∑64 PAHs in North Atlantic Ocean (24 μg m^{-2} d^{-1}) with an average F_{WD} value about 8 μg m^{-2} d^{-1} in the

global scale based on the rain samples. The apparent higher F_{WD} values of PAHs were found in urban areas of China (62.6 μg m^{-2} d^{-1}) (Wang et al., 2016) from rain samples and much lower F_{WD} values of PAHs (0.02-0.28 μg m^{-2} d^{-1}) from both rain and snow were observed in high mountain European areas (Arellano et al., 2018). Our F_{WD} values were within the range of global scale and the difference of wet deposition was mainly depended on the source distance and precipitation intensity." in **Line 427-435 Page 15-16**.

18. Line 398. Comment the range of diffusive fluxes, and show them in a figure, maybe in the supplementary material.

Response: we have added the description and graph of F_{AW} fluxes as "The estimated net diffusion of air–water exchange (F_{AW}, ng m^{-2} d^{-1}) revealed that most PAHs had net inputs from the atmosphere to ocean except for the more volatile PAHs such as 2–3 ring PAHs (Fig. 6b). The lighter PAHs (2-3 rings) appeared more volatilization trend (978-4892 ng m^{-2} d^{-1}) while heavier PAHs (4-6 rings) showed net deposition (1561-7808 ng m^{-2} d^{-1}) except for dibenzo(a,h)anthracene (1322 ng m-2 d-1), indeno(1,2,3-cd)pyrene (1238 ng m^{-2} d^{-1}), trimethylphenanthrene (1901 ng m^{-2} d^{-1}) and benzo(g,h,i)perylene (2708 ng m^{-2} d^{-1}), and three orders of magnitudes higher net deposition were observed for methylphenanthrene, dimethylphenanthrene, trimethylphenanthrene and tetramethylphenanthrene (Fig. S9). Our results were similar to the volatilization of costal water in other PAH-affected areas such as southeast Mediterranean (Castro-Jimenez et al., 2012), Narragansett Bay (Lohmann et al., 2011) and North Atlantic Ocean (Lohmann et al., 2009). Ma et al. (2013) suggested that slight volatilization of lighter PAHs may exist additional sources as ship ballast and riverine runoff, which was consistent with our study that the higher volatilization was found in East Siberian Sea and Barents Sea where more industrial factories and urban areas are situated. Our study is also consistent with previous reports in which the results showed that diffusion during air–water exchange is the main process for transfers of relatively lighter volatile organic compounds in the marine environment (Castro-Jimenez et al., 2012;Jurado et al., 2005)." in **Line 436-449 Page 16**.

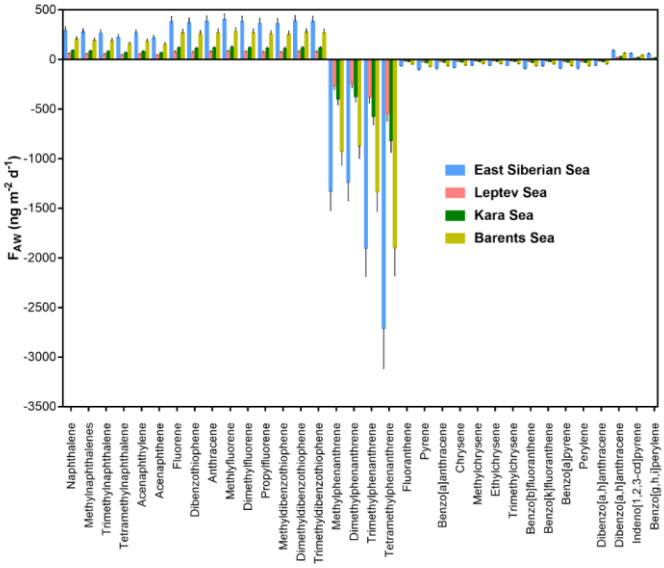

Figure S9. Estimated average net diffusive air-water exchange (FAW) of PAHs in the Russian Arctic Ocean. Bars represent standard deviation.

19. Line 399 and figure 6b. This is not clear to me. For which pahs there is a net volatilization and for which there is a net deposition.
Response: we have remade these figures as Figure 6-7.

20. Line 413. Rewrite. As I understand them, these fluxes for the the basins studied, but not all the Arctic, which should be clarified. Provide the surface for each basin in methods.
Response: we have rewritten this sentence as "This indicates that atmospheric transport of PAHs derived from anthropogenic activities is for all sectors of the Russian Arctic Ocean while only East Siberian Sea and Leptev Sea have more anthropogenic PAHs in water phase." **in line 476-478, Page 17**. We did not divide the four seas very specifically since we sampled based on ship route and we have added the island marks to divided in surface for each sea basin in the methods **in Line 113-114, Page 5**.

21. Review the spelling of pah's names in figure 4 and 5. The size of the legend (scale) in the figures should be bigger.
Response: we have checked the spelling and remade the Figures to make the legend larger.

22. Review the use of English in the manuscript.
Response: we have asked a native speaker to check the language throughout the manuscript.

23. Table S4. Why dibenzothiphene and anthracene appear twice in this table, while phenanthrene is not there? Review all the tables and data set. In addition, the mean total concentrations seem to not correspond to the distribution seen in Figure 5.
Response: thank you very much for your careful checking. Indeed, we have found that PAHs did not match the concentration data. We have checked our original dataset and have revised all tables. We also checked whether the data used in Figures are correct as shown in the tables.

24. Figure S5. The three legends appear as Cg… correct.
Response: we have corrected this term and remade the graphs.

25. Improve the quality of the figures in the supplementary material. Generally, the presentation aspects of this work need to be reviewed.
Response: thank you for your contribution. We have revised our quality of the figures in the supplementary material according to your good suggestions. We wish you continue helping us to improve our manuscript.

Atmosphere–ocean exchange of heavy metals and polycyclic aromatic hydrocarbons in the Russian Arctic Ocean

Xiaowen Ji[1,2], Evgeny Abakumov[2], Xianchuan Xie[1*]

[1] *State Key Laboratory of Pollution Control and Resource Reuse, Center for Hydrosciences Research, School of the Environment, Nanjing University, Nanjing 210093, P. R. China*

[2] *Department of Applied Ecology, Saint Petersburg State University, 16-line, 29, Vasilyevskiy Island, Saint Petersburg 199178, Russian Federation*

[*] Correspondence: Xianchuan Xie (xchxie@nju.edu.cn)

Abstract. Heavy metals and polycyclic aromatic hydrocarbons (PAHs) can greatly influence biotic activities and organic sources in the ocean. However, fluxes of these compounds as well as their fate, transport, and net input ~~in~~to the Arctic Ocean have not been thoroughly assessed. During April–November of the 2016 "Russian High Latitude Expedition", 51 air (gases, aerosols, wet deposition) and water samples were collected from the Russian Arctic within the Barents Sea, Kara Sea, Leptev Sea, and East Siberian Sea. Here, we report on the Russian Arctic assessment of the occurrence in dry and wet deposition of 35 PAHs and 9 metals (Pb, Cd, Cu, Co, Zn, Fe, Mn, Ni, and Hg), as well as the atmosphere–ocean fluxes of 35 PAHs and Hg^0. We observed that Hg was mainly in the gas phase and that Pb was most abundant in the gas phase compared with the aerosol and dissolved water phases. Mn, Fe, Pb, and Zn showed ~~apparently~~ higher levels than the other metals in the three phases. ~~According to the results for the 35 detected PAHs, t~~The concentrations of PAHs in aerosols and the dissolved water phase were ~~about~~ approximately one order of magnitude higher than those in the gas phase. The abundances of higher molecular weight PAHs were highest in the aerosols. Higher levels of both heavy metals and PAHs were observed in the Barents Sea, Kara Sea, and East Siberian Sea, which were close to areas with urban and industrial sites. Diagnostic ratios of phenanthrene/anthracene to fluoranthene/pyrene showed a pyrogenic source for the aerosols and gases, while the patterns for the dissolved water phase were indicative of both petrogenic and pyrogenic sources; pyrogenic sources were most prevalent in the Kara Sea and Leptev Sea. These differences between air and seawater reflect the different sources of PAHs through atmospheric transport, which included anthropogenic sources for gases and aerosols and mixtures of anthropogenic and biogenic sources along the continent in the Russian Arctic. The average dry deposition of $\sum_9$metals and $\sum_{35}$PAHs was 1749 ng m^{-2} d^{-1} and 1108 ng m^{-2} d^{-1}, respectively. The average wet deposition of $\sum_9$metals and $\sum_{35}$PAHs was 33.29 μg m^{-2} d^{-1} and 221.31 μg m^{-2} d^{-1}, respectively. For the atmosphere–sea exchange, the monthly atmospheric input of $\sum_{35}$PAHs was estimated at 1040 ~~tonnes~~tons. The monthly atmospheric Hg input was approximately 530 ~~tonnes~~tons. These additional inputs of hazardous compounds may be disturbing the biochemical cycles in the Arctic Ocean.

Key words: Trace metals; PAHs; Russian Arctic; atmosphere–water fluxes

1 Introduction

The increasing anthropogenic activities associated with growing industries within boundary areas of the Arctic for economic reasons, including hydrocarbon exploration sites and mines in the Russian Arctic, represent potential pollution sources to Arctic ecosystems (Walker et al., 2003; Dahle et al., 2009; Ji et al., 2019). Additionally, the Arctic has long been contaminated by pollutants transported to polar areas from distant locations outside of this region (Hung et al., 2016). For example, anthropogenic sources of pollutants in the Arctic have been found to come from the Norilsk industrial area in the Taymyr Peninsula (Reimann et al., 1997; Zhulidov et al., 2011) and from the copper-nickel mining industry in the Kola Peninsula (Boyd et al., 2009; Jaffe et al., 1995). For pollutants transported from outside of the Arctic, reducing global emissions would be an ideal strategy to lessen the impacts of pollutants on Arctic ecosystems. For example, worldwide emissions of mercury will have increased by 25% in 2020 over 2005 levels according to previous estimations ~~(Pacyna et al., 2010),~~ (Pacyna et al., 2010). ~~and m~~Mercury is a key problematic pollutant in the Arctic because it is a neurotoxic pollutant significantly influencing northern latitudes through human exposure from eating seafood and marine mammals (Stow et al., 2015). Thus, global emission reductions could help to alleviate problems associated with long-range mercury transport and contamination in the Arctic. In regard to sources close to the Arctic, these may inevitably cause localized ecological risks or risks over a wider regional range. For instance, Fernandes and Sicre (1999) showed that atmospheric transport of anthropogenic polycyclic aromatic hydrocarbons (PAHs) to the Eurasian Arctic mainly originated from Eastern Europe and Russia. PAHs in aerosols from lower latitude were deposited on soils and ice in winter and transported by rivers to the ocean by the occurrence of freshet (Fernandes and Sicre, 1999). The previous study also showed a strong net deposition in the marine transect from East Asia to the Arctic, and the controlling sources both contained potential continental source region as East Asia and the influence of seasonal and regional source as forest fires in the Arctic (Ma et al., 2013). In addition, high concentrations of heavy metals (Mn, Zn, Ni, Fe and Cd) were observed in the west Arctic Ocean (Chukchi Sea); this enrichment was not only from Pacific-origin inflow water from the Bering Stat but also from additional sources such as melting sea ice and river water discharge (Kondo et al., 2016). Also of concern is that, with rapid warming of the global climate, the melting of contaminated ice may lead to more pollutant emission into the Arctic Ocean, which could harm its fragile ecosystems.

Pollutants can be transported to the Arctic through both seawater and atmospheric pathways~~, and;~~ the atmospheric pathway is the quickest and most direct way for long-range pollutant transportation, e.g., pollutants can be transported from distant sources to the Arctic within several days or weeks ~~via this pathway~~ (Shevchenko et al., 2003). Reports have revealed that some pollutants such as heavy metals and polycyclic aromatic hydrocarbons (PAHs) can be transported with aerosols over thousands of kilometers to Arctic regions (Rahn and Lowenthal, 1984; Maenhaut et al., 1989; Shaw, 1991; Cheng et al., 1993). Approximately 100 ~~tonnes~~ tons ~~per year~~ of airborne mercury originating from industrial sources are deposited per year in the Arctic Ocean (Cone, 2008). While there is evidence that atmospheric inputs make large contributions to the chemical budgets in marine areas, the exact role of these inputs in the Arctic Ocean remains uncertain and may have been previously underestimated (Duce et al., 1991). Numerous studies have ~~proven~~ shown that aerosol transport is ~~an important way in which~~essential to transfer atmospheric compounds ~~are transferred~~ from air to ocean ~~water~~, and that this process is susceptible to changes ~~of~~ in the climate ~~in~~ of Arctic regions (Leck et al., 1996; Sirois and Barrie, 1999; Bigg and Leck, 2001). The compounds in aerosols over the Russian Arctic have been reported to show maximal concentrations during the winter/spring season~~,~~; in addition, ~~and~~ 50% of the air pollutants were found to have originated from Russian Arctic pollution ~~itself~~ (Shevchenko et al., 2003). It has also been reported that the natural biodegradation rates of exogenous compounds in the Arctic Ocean could be lower than those in more temperate oceans such as the Atlantic and Pacific (Bagi et al., 2014). In addition, Vieira et al. (2019) found that ~~some metals (~~Fe, Mn, and Co~~)~~ were predominantly controlled~~altered~~ by reductive benthic inputs, and that their levels were affected by the biological processes of uptake and release in the Arctic Ocean. Because of their toxicity and persistence, high concentrations of heavy metals or other persistent pollutants such as PAHs may disturb the benthic fluxes in cross-shelf mixing in Arctic regions, which could result in adverse effects on marine life~~,~~ and, with the eventual biomagnification in the food web, on humans ~~could be affected~~ as well. However, ~~, up to now, there has been an insufficient understanding of how these compounds (~~the long-term influence of heavy metals and PAHs~~) participate in~~ on biogeochemical cycles ~~over the long term~~ in the Arctic Ocean remains poorly understood.~~.~~

~~The a~~Atmosphere–seawater exchange is the ~~major~~ main process that controls the residence time and levels of chemical compounds in the Arctic Ocean. In particular, atmospheric deposition is a significant source for pollutants in seawater, and dry deposition in ~~different~~ the ocean~~s~~ has been widely studied (Jickells and Baker, 2019; Wang et al., 2019; Park et al., 2019). Although wet deposition (precipitation scavenging) is regarded as playing a predominant role in eliminating pollutants in both gas and particulate phases, current reports on the spatial distribution of pollutants from wet(snow) deposition in high-latitude oceans are scarce (Custódio et al.,

2014). Moreover, for volatile or semivolatile compounds, the volatilization process is an important pathway for atmosphere–seawater exchanges. Therefore, the atmosphere–water exchange of volatile or semivolatile compounds can be estimated by the net flux of pollutants either volatilizing from seawater to air or depositing from air to seawater (Rasiq et al., 2019; Cheng et al., 2013; Totten et al., 2001). Gonzalez-Gaya et al. (2016) reported on a global assessment of atmosphere–ocean fluxes of 64 PAHs; ~~and~~ the net atmospheric PAH input to global ocean was 0.09 Tg per month ~~to the global ocean~~. ~~It is undeniable that t~~The atmosphere–seawater exchange rate is greatly influenced by atmospheric temperature variations, and the direction and magnitude of fluxes of compounds between air and seawater vary seasonally (Bamford et al., 1999; Hornbuckle et al., 1994). Additionally, ~~for organic compounds as PAHs,~~ inorganic salt ions can decrease the aqueous solubility of organic compounds such as PAHs (Rasiq et al., 2019). During ~~the period of~~ melting of sea ice in the Arctic Ocean, the magnitude and direction of atmosphere–seawater fluxes may be different from those in tropical and subtropical oceans (Gonzalez-Gaya et al., 2016; Rasiq et al., 2019). ~~Although t~~The Arctic Ocean is considered as a sink that receives global airborne pollutants ~~(Environment Canada; et al., 2008),~~ (Environment-Canada; et al., 2008); ~~unfortunately~~however, the ~~characteristics~~ fate of atmosphere–ocean exchange~~s~~ of trace metals and organic compounds ~~have~~ remain~~ed~~ unclear ~~up to now~~.

In this study, ~~with the Arctic Ocean as the research area,~~ two categories of pollutants (i.e., 9 heavy metals and 35 PAHs) were measured in the Arctic Ocean, in aerosols, gas, and seawater, and atmosphere–ocean exchanges of Hg and PAHs ~~were~~ was studied. We hypothesized about the relative equilibrium of chemical exchanges between seawater and air and calculated the net diffusion of atmosphere–ocean exchange of Hg and PAHs in the Arctic Ocean for an evaluation of the double-directional exchange. Meanwhile, the dry and wet deposition of heavy metals and PAHs in the Russian Arctic Ocean were determined. The distributions of heavy metals and PAHs in each sea of the Arctic Ocean and in ~~different~~ various phases were also characterized to identify possible sources from the continents.

2 Materials and methods

2.1 Study area and sample collection

All samples were collected during the period of ~~9th~~ April 9 to ~~10th~~ November 10, ~~of~~ 2016 as part of the "Russian High Latitude Expedition" carried out on the vessel *Mikhail Somov* (this vessel traveled from the ~~City~~ city of Arkhangelsk to Wrangel Island). Fifty-one air and water samples, and eight wet deposition samples were gathered from locations ranging from the southern inlet of the Barents Sea (from west sites to Vayach

Island) to across the Kara Sea (to Gerkules Island), Laptev Sea (to Bennett Island), and East Siberian Sea (to Wrangel Island) (**Fig. 1**).

2.1.1 Aerosol and gas phase

Air samples, including aerosols and concurrent gases as described elsewhere (Reddy et al., 2012; Shoeib and Harner, 2002; Galarneau et al., 2017; Grosjean, 1983; Wu, 2014), were collected by a high-volume sampler set up at the top of a main rod. A wind vane was connected to the high-volume sampler so that samples could be collected only if the wind was derived from the bow to prevent contamination from ship emissions. The average sampled air volume was 632 m^3 (412–963 m^3) per sample. The aerosols were sampled on Teflon filters (P0325-100EA, Fluoropore, Darmstadt, Germany), and then, the compounds in the gas phase were collected over precleaned polyurethane foams (PUFs). After sampling, the filters and PUFs were ~~placed~~ tightly covered with aluminum foil for air-tightness, then immediately placed in polyethylene bags,~~in polyethylene bags, covered with aluminum foil,~~ and frozen at -20 °C prior to chemical analyses.

2.1.2 Wet deposition and water

Wet deposition samples were collected through a cleaned stainless steel funnel connected to a glass bottle during eight snow events. Snowfall samples were melted thoroughly at room temperature. Water samples were gathered continuously from surface seawater (5 m depth) along the vessel, and these samples were immediately filtered onto borosilicate microfiber glass filters (AP1504700, EMD Millipore, Darmstadt, Germany). Then, the compounds in the dissolved phase were retained on XAD sorbent tubes subjected to controlled flows. The mean filtered water volume was 1239 ~~m^3~~ mL (135–2876 ~~m^3~~ mL). The XAD tubes were stored at 5 °C before their extraction in the laboratory.

设置了格式: 非上标/ 下标

设置了格式: 非上标/ 下标

2.2 Heavy metal extraction and analysis

For ~~the~~ metal determinations in the aerosol, gas phase, wet deposition, and water samples, Teflon filters, PUFs, and dissolved phases were first Soxhlet-extracted for 8 h by using HNO_3~~, and then,~~. T~~t~~he samples were then diluted with deionized water to 23 mL and subjected to inductively coupled plasma mass spectrometry (ICP-MS) analysis. Specifically, the contents of Pb, Cd, Cu, Co, Zn, Fe, Mn, Ni, and Hg were analyzed on an ICP-MS instrument (Thermo Scientific ICE 3500, Waltham, MA, USA) while making use of rhodium (Rh) as an internal standard. High-resolution (10,000) data were collected to avoid any mass interference problems.

2.3 PAH extraction and analysis

For ~~the~~ PAH determinations in the gas, aerosol, and dissolved phase samples, published procedures were used (Berrojalbiz et al., 2011; Castro-Jimenez et al., 2012; Gonzalez-Gaya et al., 2014). Snow-melt water was extracted by using solid phase HLB Oasis cartridges (60 mg/3 cc) on board. Briefly, cartridges were preconditioned with 5 mL methanol, 10 mL of a mixture of methanol:dichloromethane (1:2), and 10 mL deionized water. Afterward, each sample was combined with a recovery standard and concentrated by N_2 until near dryness. Then, it was eluted with 5 mL hexane, 5 mL of a mixture of hexane:dichloromethane (1:2), and 10 mL deionized water.

Thirty-five PAH species were quantified, including naphthalene, methylnaphthalene (sum of two isomers), 1,4,5-trimethylnaphthalene, 1,2,5,6-tetramethylnaphthalene, acenaphthylene, acenaphthene, fluorene, dibenzothiophene, anthracene, 9-methlyfluorene, 1,7-dimethylfluorene, 9-n-propylfluorene, 2-methyldibenzothiophene, 2,4-dimethyldibenzothiophene, 2,4,7-trimethyldibenzothiophene, 3-methylphenanthrene, 1,6-dimethylphenanthrene, 1,2,9-trimethylphenanthrene, 1,2,6,9-tetramethylphenanthrene, fluoranthene, pyrene, benzo[*a*]anthracene, chrysene, 3-methylchrysene, 6-ethylchrysene, 1,3,6-trimethylchrysene, benzo[*b*]fluoranthene, benzo[*k*]fluoranthene, benzo[*a*]pyrene, perylene, dibenzo[*a,h*]anthracene, indeno[*1,2,3-cd*]pyrene, dibenzo[*a,h*]anthracene, and benzo[*g,h,i*]perylene. ~~The~~ PAH quantification was performed ~~with~~ by gas chromatography-mass spectrometry (GC-MS). Specifically, we used a gas chromatograph coupled with a triple quadrupole mass selective detector (GS-MS, ITQ 1100, Thermo Scientific, USA) equipped with a DB-5MS chromatographic capillary column (30 m × 0.25 mm i.d. and 0.25-µm film, Agilent Technologies, Santa Clara, CA, USA) operating in electron impact mode (EI) and with selected ion monitoring (SIM) as reported ~~before~~ previously (Gonzalez-Gaya et al., 2014). ~~The i~~Internal standards (anthracene-d_{10}, *p*-terphenyl-d_{14}, pyrene-d_{10}, and benzo[*b*]fluoranthene-d12) were added before operating the GC-MS instrument for the quantification of PAHs, and the recovery of perdeuterated standards (acenaphthene-d_{10}, chrysene-d_{12}, phenanthrene-d_{10}, and perylene-d_{12}) was determined by addition prior to the procedures of extraction; these values were then used for the correction of measured concentrations.

2.4 Quality assurance and quality control

Analyses of every sample and phase were conducted in the laboratory with field blanks to determine the analytical limits and recoveries. Breakthroughs of aerosols and gas phases were checked for the Teflon filter and PUF samples. Approximately 90% of the metals and PAHs were obtained during the first half of the sample analysis, while the remaining 10% were obtained during the second half; for the PAHs, these mostly consisted of compounds with 2–3 rings. Six blanks (field and laboratory) were collected for the gas phase, while ~~for the dissolved phase,~~ seven field banks and eight laboratory blanks were used for the dissolved phase,

all of which were extracted along with the rest of the samples during the analytical procedure. For the gas phase, average ∑metal values were approximately 0.049 and 0.052 ng per sample in the field and laboratory blanks, respectively, and average ∑PAH values were approximately 2.44 and 2.06 ng per sample in the field and laboratory blanks, respectively (**Table S1 and S2, Supplementary material**). For the aerosols, average ∑metal values were 0.046 and 0.065 ng per sample in the field and laboratory blanks, respectively, and average ∑PAH values were 2.95 and 2.96 ng per sample in the field and laboratory blanks, respectively. Likewise, for the dissolved phase, values of 0.053 and 0.052 ng per sample were obtained for the ∑metals and values of 2 and 1.73 ng per sample were obtained for the ∑PAHs. All measured PAHs from field samples exceeded the field and laboratory blank concentrations; therefore, the quantified compounds did not~~were not~~ subtract~~ed by those values~~ the blank values. Mean recoveries of perdeuterated standards used as surrogates in dissolved samples were as follows: 63% for acenaphthene-d_{10}, 54% for chrysene-d_{12}, 73% for phenanthrene-d_{10}, and 82% for perylene-d_{12}.

All concentrations in each medium were corrected by the surrogate recovery for individual samples. The detection limit was used for the lowest limit of the calibration curve. The quantification limit was equivalent to the average blank concentration for each phase.

2.5 Data processing

Dry deposition fluxes (F_{DD}, ng m^{-2} d^{-1}) were calculated from field measurements of trace metals and PAHs collected during the expedition over eight time periods. Aerosol deposition fluxes for the metals were calculated as ~~shown in Eq. (1)~~follows:

$$F_{DD}(metal) = C_d V_d \quad (1)$$

where C_d is the concentration of atmospheric aerosols and V_d is the velocity of deposition (m s^{-1}). V_d was calculated as shown in Eq. (2), and the details have been described elsewhere (Zhang et al., 2001):

$$V_d = u_{grav} + \frac{1}{R_a + R_s} \quad (2)$$

where u_{grav} is the gravitational settling velocity and R_a and R_s are the aerodynamic resistance for gaseous species and the surface resistance, respectively. R_s can be calculated as follows:

$$R_s = \frac{1}{\varepsilon_0 u_* (E_B E_{IM}) R_1} \quad (3)$$

where ε_0 is an empirical constant (ε_0 = 3) and u_* is the friction velocity calculated for gases. E_B is the collection efficiency of Brownian diffusion as a function of the Schmidt number Sc:

$$E_B = (Sc)^{-\gamma} \quad (4)$$

where γ is an empirical constant (γ = 0.5). E_{IM} is the collection efficiency from impaction based on the following formulas (Peters and Eiden, 1992):

$$E_{IM} = \left(\frac{st}{0.8 + st}\right)^2 \quad (5)$$

$$st = \frac{V_{grav} V_*^2}{V_a} \quad (6)$$

where V_a is the kinematic viscosity for air ($m^2\ s^{-1}$). The correction factor (R_1) is the fraction of particles close to the surface:

$$R_1 = exp(-st^{1/2}) \quad (7)$$

For PAHs, the specific compound deposition velocity (V_d, cm s^{-1}) was derived from an empirical parameterization (Gonzalez-Gaya et al., 2014):

$$\log(V_d) = -0.261\log(P_L) + 0.387U_{10}Chl_s - 3.082 \quad (8)$$

where P_L is the subcooled liquid vapor pressure of each PAH, U_{10} is the 10 m height wind speed, and CHl_s is the concentration of surface chlorophyll. With Eq. (8), one can estimate the V_d for each PAH and sampling period by taking P_L from references and using the field-measured U_{10} and CHl_s. In this study, F_{DD}(PAH) values were estimated ~~by~~ from the measured concentrations ~~of~~ in the aerosol phase (C_A, ng m^{-3}) ~~by using~~as follows:

$$F_{DD}(PAHs) = 864V_dC_A \quad (9)$$

where 864 is the unit conversion factor.

The wet deposition fluxes (F_W, ng m^{-3} d^{-1}) of metals/PAHs were estimated by using the quantified concentrations of metals/PAHs from the collected snow and the precipitated volume of snow-melt water per surface and time period for each of the eight snow events during the expedition.

The air–water diffusive fluxes (F_{AW}, ng m^{-2} d^{-1}) for Hg/PAHs were calculated according to Fick's law:

$$F_{AW} = K_{AW}\left(\frac{C_G}{H'} - 1000C_{TW}\right) \quad (10)$$

where C_G and C_{TW} represent the concentration measured in the gas phase (ng m^{-3}) and dissolved phase (ng L^{-1}), respectively. H' is the temperature dependence of Henry's law constant, and H' values for PAHs were taken from Bamford et al. (1999)~~elsewhere (Bamford et al., 1999)~~; H' for Hg was calculated from Eq. (11) for seawater (Andersson et al., 2008) ~~proposed by Andersson et al. (2008)~~:

$$H' = exp\left(\frac{-2404.3}{T} + 6.92\right) \quad (11)$$

where T is the temperature of the surface water (K). H' was corrected by the field-measured salinity. K_{AW} represents the air–water mass transfer rate (m d^{-1}) calculated by a two-film model (Singh and Xu, 1997) and

while considering the nonlinear wind-speed effect. C_{TW} for Hg was ~~calculated with~~ directly measured concentrations, and C_{TW} values for PAHs were calculated by using the measured concentrations in the dissolved phase (C_W) as follows:

$$C_T = \left(\frac{C_W}{1 + k_{DOC}DOC}\right) \quad (12)$$

where K_{DOC} was taken as the value of 10% of the octanol–water partitioning coefficient (K_{OW}) (Burkhard, 2000), and DOC represents the dissolved organic carbon (mg L^{-1}).

K_{AW} was calculated by the two-film model:

$$\frac{1}{K_{AW}} = \frac{1}{K_W K_A H} \quad (13)$$

where K_W and K_A are the mass transfer coefficients (m d^{-1}) of Hg and PAHs in the water and air films, respectively. ~~CO_2 in the water phase of t~~The mass transfer coefficient of CO_2 in the water phase (K_{W,CO_2}, m d^{-1}) can be used to calculate K_W (Gonzalez-Gaya et al., 2016), which is a wind-speed quadratic function at a height of 10 m (U_{10}, m^{-1}) (Nightingale et al., 2000). A Weibull distribution of wind speed was assumed to parameterize K_{W,CO_2} because average wind speeds were used during the sampling period since the gas and dissolved phase concentrations were averaged values for the sampling transects; K_{W,CO_2} was calculated by using a previously reported method (Livingstone and Imboden, 1993):

$$K_{W,CO_2} = 0.24[0.24\eta^2\Gamma\left(1 + \frac{2}{\xi}\right) + 0.061\eta\Gamma(1 + 1/\xi)] \quad (14)$$

where η and ξ are the constants of scale and shape in the Weibull distribution, respectively, and Γ represents a gamma function. ξ = 2 (Rayleigh distribution) was used as recommended (Gonzalez-Gaya et al., 2016). η is related to ~~the~~ wind speed~~s~~ and was calculated with $U_{10} = \eta\Gamma(1 + 1/\xi)$ (Livingstone and Imboden, 1993).

K_W can be calculated ~~by~~as follows:

$$K_W = K_{W,CO_2}\frac{1}{\sqrt{\frac{SC_{PAH}}{600}}} \quad (15)$$

where SC_{PAH} is the Hg/PAH Schmidt number. The same applies for K_A, which was also calculated ~~on the basis of~~from wind speed~~s~~ and ~~by using~~ the H_2O mass transfer coefficient for the air phase (K_{A,H_2O}, cm s^{-1}):

$$K_{A,H_2O} = 0.2U_{10} + 0.3 \quad (16)$$

$$K_A = 864K_{A,H_2O}\sqrt{\frac{D_{i,a}}{D_{H_2O,a}}} \quad (17)$$

where $D_{i,a}$ and $D_{H_2O,a}$ represent the Hg/PAH and H_2O diffusive coefficients in air, respectively.

The uncertainty was lower than a factor of one to two in these estimates for metals/PAHs. Most of the increasing uncertainty was associated with the Henry's law constants. The effect of uncertainty on the air–water exchange net direction was assessed by the ratios of air–water fugacity (f_G/f_W) (**Figs. S1 and S2, Supplementary material**~~),~~); moreover, and the findings revealed that most metals and PAHs were not close to the equilibrium of air–water. Among the PAHs, net volatilization was detected only for dibenzothiophene, alkylated phenanthrenes, and fluoranthene. The details of the uncertainty analysis are shown in **Text S1 (Supplementary material)**.

设置了格式: 字体: 加粗

设置了格式: 字体: 加粗

Gross fluxes of volatilization and absorption depend on the first and second term of Eq. (10). The total accumulated fluxes for the Barents Sea, Kara Sea, Laptev Sea, and East Siberian Sea were acquired by multiplying the mean basin flux with ~~the~~ its standard deviation by the surface area of each basin.

The estimations of degradation fluxes of PAHs in the atmospheric ocean boundary were calculated as follows:

$$D_{atm} = \frac{(C_{Gf} - C_{Gi})ABL}{t} \quad (18)$$

where C_{Gf} and C_{Gi} are the last concentration after a fixed time in a closed system (ng m^{-3}) and the concentration in the gas phase at the initial time (ng m^{-3}), respectively. t is the time period (average 5 h daytime per day), and ABL represents the average height of the atmospheric boundary layer (380 m). C_{Gf} can be calculated as follows:

$$Ln(\frac{C_{Gi}}{C_{Gf}} = k_{OH}[OH]t) \quad (19)$$

where k_{OH} is the rate constant for a PAH reaction with OH radicals (Keyte et al., 2013) and [OH] is the hydroxyl radical concentration in the mixed layer (1000–500 hPa) based on the monthly mean OH radical concentration (Spivakovsky et al., 2000). The mean concentrations of OH were calculated by Eq. (13). The OH concentrations ranged between 5.23 and 17.26 × 10^5 mol cm^{-3}. Besides, only the PAHs in the gas phase were considered while the potential degradation of PAHs bound in aerosols was ignored. Considering the uncertainty of those sources, a relevant error factor of ~~two to three~~2-3 was given ~~in the figure~~ for the degradative fluxes based on the individual PAHs. Because of the large uncertainties in k_{OH} values, the degradation fluxes of PAHs in the atmosphere could not be ~~provided~~calculated.

3 Results and discussion

3.1 Heavy metals in the atmosphere-ocean

Nine heavy metals were measured, and ~~each metal's~~the average concentration for each metal in each sea can be found in **Table S3**. The highest $\sum_9$ metal concentrations in the Barents Sea were found in the gas phase (C_G, ng m^{-3}), where the average concentration was 0.418 ng m^{-3} (**Fig. S3**). The average values of C_G showed no obvious differences among the four seas, whereas the oceanic area adjacent to the Chukchi Peninsula, Taymyr-Gydan Peninsula, and Arkhangelsk region showed higher combined concentrations of the nine metals (**Fig. 2a**). High $\sum_9$ metal concentrations in the aerosol phase (C_A, ng m^{-3}) were observed in the Barents Sea ($p < 0.05$), where the average $\sum_9$ metal concentration was 2.713 ng m^{-3} (**Fig. 2b**). These high levels may have been associated with the trajectories of air from the ~~continent of~~ Russian inlands. The distributions of heavy metals in the Russian Arctic Ocean revealed that the concentrations of the $\sum_9$ metals in seawater were lower than those in air. The concentrations of each metal in aerosols were comparable to those previously reported in the Russian Arctic, i.e., Leptev Sea, Kara Sea, Barents Sea, Sevenaya Zemlya, and Wrangel Island (Shevchenko et al., 2003; Vinogradova and Ivanova, 2017). For other parts of the Arctic Ocean, the average mass concentrations of each metal from Svalbard, the Fram Strait, Central Arctic, and Greenland (Ferrero et al., 2019; Maenhaut et al., 1979; Maenhaut et al., 2002; Maenhaut et al., 1989), were higher than those found in aerosols in our study. Metals' concentrations in aerosols in our study are lower than those in the Red Sea and Mediterranean area (Chen et al., 2008). The average $\sum_9$ metal concentrations in dissolved water (C_W~~, ng L^{-1}~~) ranged from 0.526 to 0.896 μg L^{-1} (Leptev Sea to Barents Sea). This is relatively lower than the concentrations of dissolved trace metals (Mn, Fe, Ni, Zn and Cd) previously reported for the western Arctic Ocean (Chukchi Sea and Canada Basin, depth: 5–20 cm) (Kondo et al., 2016). ~~Obviously h~~Higher values of C_W were observed in the Barents Sea–Kara Sea region (Yamal Peninsula) and in the East Siberian Sea (close to the Chukchi Peninsula) in comparison to the C_W values in other areas (**Fig. 2c**).

The abundance of each metal in gases, aerosols, and dissolved water is dependent on the emission sources. In this study, Fe and Zn were the most abundant metals detected in aerosols and dissolved water from the Russian Arctic Ocean, where the average $\sum_9$ metal concentrations in aerosols and dissolved water were 0.64 ng m^{-3} and 0.91 ng L^{-1}, respectively. Pb was the most abundant metal in the gas phase (the average concentration in the Russian Arctic Ocean = 0.14 ng m^{-3}). In comparison to aerosols and dissolved water, the gas phase contained higher ~~portions~~ levels of Hg, which is a finding consistent with the usual form of Hg in the atmosphere (>98%) and the tendency for the remaining types of Hg to adsorb to particles during atmospheric transport (Poissant et al., 2008). In all phases, the proportions of Mn, Fe, Pb, and Zn were significantly higher than those of other heavy metals. Additionally, the metal distributions in the Barents Sea and Kara Sea showed

the highest proportions, followed by the metal distributions in the East Siberian Sea. On the Taymyr Peninsula (adjacent to the Kara Sea and Leptev Sea), there is a mining and metallurgical factory operated by the company Norilsk that processes copper and nickel~~,~~ and ~~it~~ is one of the biggest metallurgical factories in the world. This may be a likely source of metals in the Kara Sea region (Shevchenko et al., 2003). Because of the significant differences in the concentrations of metals in the marine boundary layer both temporally and spatially throughout the Russian Arctic Ocean (Vinogradova and Polissar, 1995; Shevchenko et al., 1999), as well as the scarcity of reported data on heavy metals in the atmosphere ~~of~~ in this region, it was difficult to compare our data with historical findings. However, our data are similar to those reported ~~in~~ for September ~~of~~ 1993 in the Kara Sea (Rovinsky et al., 1995).

The dry deposition ~~flux~~ that involves aerosols binding to heavy metals (F_{DD}, ng m^{-2} d^{-1}) is a major process for heavy metal deposition (Shevchenko et al., 2003). In the Russian Arctic Ocean, the average F_{DD} of the $\sum_9$ metals ranged from 392 to 8067 ng m^{-2} d^{-1} (mean = 1792 ng m^{-2} d^{-1}). The largest F_{DD} value was found close to the coast of the East Siberian Sea, where F_{DD} values of 305 and 224 ng m^{-2} d^{-1} were observed for Hg and Pb, respectively, and were dominant ~~and values of 305 and 224 ng m^{-2} d^{-1}, respectively, were observed~~ (**Fig. 3a**). Our results seem to be one magnitude higher than those in the Red Sea (mean = 615 ng m^{-2} d^{-1}) (Chen et al., 2008) and Mediterranean Sea (mean = 264 ng m^{-2} d^{-1}; Chen et al. 2008~~(Chester et al.)~~) ~~(Chester et al., 1999)~~. However, this comparison may not reflect the strength of the emission sources because dry deposition is highly dependent on the deposition velocity, which is affected by meteorological conditions such as the humidity, wind speed, and stability of the air column (Mariraj Mohan, 2016). The relative humidity in the Arctic Ocean tends to be higher in coastal areas and notably we sampled during spring–winter when water vapor evaporates from the relatively warmer surfaces of seawater (Vihma et al., 2008). ~~Also~~In addition, the wind over sampling sites in the Arctic Ocean was ~ ~~approximately~~ 7 m s^{-1} on average (the largest average wind speed was ~~about~~ 9 m s^{-1} in the Barents Sea), which ~~was~~ is significantly higher than the wind in the Red Sea and Mediterranean Sea (0.36–1 m s^{-1}) (Chen et al., 2008; Chester et al., 1999). During the eight snow events encountered during the expedition, the wet deposition flux of the $\sum_9$ metals (F_{WD}, μg m^{-2} d^{-1}) ranged from 23 to 32 μg m^{-2} d^{-1} (mean = 26 μg m^{-2} d^{-1}) (**Fig. 4a**). Data relevant to the wet deposition flux of heavy metals in the Arctic region include results for Hg, which ~~was~~ were estimated on land in Alaska ~~and~~; the highest deposition was detected along the southern and southeastern coasts (~~exceeding~~ > 0.05 μg m^{-2} d^{-1}) ~~(Pearson et al., 2019);~~ (Pearson et al., 2019). T~~t~~he values were quite similar to the F_{WD} for Hg in our ~~results~~ study (0.05 to 0.09 μg m^{-2} d^{-1}). Through analysis of variance tests, we did not find any significant difference in the F_{WD} at different locations ($p > 0.05$) for all heavy metals, while a relatively higher F_{WD} for Hg was observed in coastal areas adjacent to the Taymyr

Peninsula with industrial factories. Pearson et al. (2019) pointed out that there are larger contributions from Hg wet deposition in the Bering Sea and Gulf of Alaska, which are influenced by the western Pacific downwinds of East Asia, where high Hg emissions from industrial activities and coal burning occur (Wong et al., 2006). The Russian Arctic Ocean is also affected by Pacific downwinds, which could lead to a combination of heavy metal deposition from both local anthropogenic sources and long-range transport from Asia. Wet deposition is an important process for the transfer of heavy metals from gas and aerosol phases to ocean water. Snowfall in the Arctic is an important fraction of precipitation, but variations in measurements ranging from 20% to 50% can occur ~~during~~ under windy conditions even with sampling equipment designed with wind protection (Rasmussen et al., 2012). However, snow events are quite sporadic in the Russian Arctic Ocean during spring–summer compared with the other deposition processes. Nevertheless, ~~the~~ wet deposition in our study was under regional influences and had ~~as~~ relatively high uncertainty ~~and is under regional influences~~.

For many heavy metals that form volatile species, there is additional evidence that their existence in water is strongly related to releases from terrestrial environments rather than internal cycling in aquatic systems (Robert, 2013). For example, following the deposition of atmospheric Fe, a non-volatile species, the concentrations in water are influenced mainly by the particulate phase and its dissolution, whereas for Hg, a volatile species that predominantly exists in the atmosphere as a gas (Hg^0), the concentrations of volatile Hg species in water are largely influenced by volatilization and deposition processes at the air–water interface; portions of the Hg in aquatic systems ends up being converted to methylmercury (Mason and Sheu, 2002; Sunderland and Mason, 2007; Selin et al., 2007; Strode et al., 2007). Hg concentrations in the gas phase in the present study were significantly lower than those measured in 1996 in the Northern Hemisphere (1.5–1.7 ng m^{-3}) and Southern Hemisphere (1.2–1.3 ng m^{-3}) (Steffen et al., 2005; Slemr et al., 2003; Wängberg et al., 2007; Kim et al., 2005). Steffen et al. (2002) indicated that there has been increasing retention of Hg in the Arctic region based on analyses of long-term measurements of atmospheric Hg concentrations. Diffusive air–water exchange is the dominant process driving the exchange of Hg in the ocean. The net diffusive air–water exchange (F_{AW}, ng m^{-2} d^{-1}) was estimated by a two-film resistance model (Robert, 2013). The net input of Hg was calculated as shown in **Fig. 3b**~~,~~ and ~~the results~~ revealed that there was a net input from the atmosphere to the ocean at all stations, especially for the stations close to industrial/urban areas. The integrated monthly F_{AW} fluxes (ton~~ne~~s per month) for Hg were of the same order of magnitude as the F_{DD} fluxes for Hg and other heavy metals in the Russian Arctic Ocean (**Fig. S4**). For Hg, the gross volatilization and gross absorption in the Russian Arctic Ocean were 250 ~~tonnes per month~~ and 530 ~~tonnes~~ tons per month, respectively. In consideration of previous studies ~~concerning~~ of atmospheric mercury depletion events (AMDEs), during which the net input

of Hg in the Arctic was evaluated (Brooks et al., 2006; Lindberg et al., 2001), we adjusted our sampling times to avoid sampling during sunrise when the autocatalytic release of sea salt aerosols changes the oxidative photochemistry in the stratified planetary boundary layer where elemental and reactive Hg in the gas phase is oxidized by reactive halogens. It was estimated that ~~about~~ 99 ~~to~~ 496 ton~~ne~~s of Hg are deposited per year in the Arctic during AMDEs (Skov et al., 2006; Ariya et al., 2004). The net input of Hg in ~~this~~ the present study was ~~apparently~~ one order of magnitude higher than that caused by the AMDEs~~, and~~ ; this discrepancy may ~~have been related to~~result from the fact that the previous studies ~~were estimated based on~~considered the terrestrial boundary between air masses and snowpack, and that the different locations and seasons were affected by different meteorological conditions. In northern regions, it has been shown that Hg undergoes long-range transport from Eurasia, especially during the winter season (Poissant et al., 2008). These net amounts of Hg entering into the Arctic Ocean pose potential risks to marine biota because Hg is poorly mobile and can be retained by aquatic biota that are exposed to it~~the Hg~~ during the deposition process (Harris et al., 2007).

3.2 PAHs in the atmosphere-ocean

Thirty-five individual PAHs, which included isomer groups such as alkylated PAHs, were measured. The average concentrations of PAHs in each sea of the Russian Arctic Ocean are shown in **Table S4**. The average values of C_G showed no obvious differences in the Kara Sea, Laptev Sea, and East Siberian Sea ($p > 0.05$), and no particularly high levels of C_G were detected at all of the sampling sites (**Fig. 5a**). The range of $\sum_{35}$ PAH C_G is 19.87–22.14 ng m_a^{-3} for the Barents Sea, 19.01–22.34 ng m_a^{-3} for the Kara Sea, 19.23–21.70 ng m_a^{-3} for the Leptev Sea, and 19.28–22.61 ng m_a^{-3} for the East Siberian Sea. The highest C_G of $\sum_{35}$ PAH is observed in the Barents Sea, with a value of 22.61 ng m_a^{-3}. $\sum_{35}$ PAH C_A in the Barents Sea (0.25–2.95 ng m_a^{-3}), and East Siberian Sea (0.24–3.32), with average values of 1.38 and 2.07 ng m_a^{-3} , respectively, were higher than those in the Leptev Sea (0.23–0.89 ng m_a^{-3}) and Kara Sea (0.23–0.27 ng m_a^{-3}), with average ~~CA~~ values of 0.30 and 0.25 ng m_a^{-3}, respectively (**Fig. 5b**). The average C_A of $\sum_{35}$ PAH in the present study is higher than ~~those~~ the average C_A of $\sum_{64}$ PAH measured in the South Atlantic Ocean (~~mean =~~ 0.93 ng m_a^{-3}) and North Pacific Ocean (~~mean =~~ 0.56 ng m_a^{-3}), while much lower than the ~~those~~ average C_A of $\sum_{64}$ PAH in the Indian Ocean (~~mean =~~ 10 ng m_a^{-3}) (Gonzalez-Gaya et al., 2016)~~(Gonzalez-Gaya et al., 2016). Considering~~ The average $\sum_{35}$ PAH C_A of ~~(~~1.02 ng m_a^{-3}~~)~~ in the Russian Arctic Ocean~~, the value~~ is comparable to ~~those of~~ the average $\sum_{64}$ PAH C_A observed in the South Atlantic Ocean and South Pacific Ocean (~~both mean =~~ 1.1 ng m_a^{-3}) (Gonzalez-Gaya et al., 2016)~~(Gonzalez-Gaya et al., 2016). The levels of~~ $\sum_{18}$ PAH C_A was~~ere was~~ measured from the North Pacific towards the Arctic Ocean, ~~with the range~~ranging from 0.0002 to 0.36 ng m_a^{-3}, with the highest concentration found in the coastal areas in East Asia~~-~~ (Ma et al., 2013)~~(Ma et al., 2013).~~ These concentrations were

设置了格式: 下标
设置了格式: 下标
设置了格式: 上标
设置了格式: 上标
设置了格式: 上标
设置了格式: 上标
设置了格式: 下标
设置了格式: 下标
设置了格式: 上标
设置了格式: 下标
设置了格式: 下标
设置了格式: 上标
设置了格式: 上标
设置了格式: 上标
设置了格式: 上标
设置了格式: 上标
设置了格式: 字体: 加粗
设置了格式: 下标
设置了格式: 下标
设置了格式: 下标
设置了格式: 下标
设置了格式: 上标
设置了格式: 上标
设置了格式: 下标
设置了格式: 下标
设置了格式: 上标
设置了格式: 下标
设置了格式: 下标
设置了格式: 上标
设置了格式: 下标
设置了格式: 下标
设置了格式: 上标
设置了格式: 下标
设置了格式: 下标
设置了格式: 上标

significantly lower than the ~~average~~averages levels found in our study. Besides, Ma et al. (2013) ~~Ma et al. (2013)~~ observed the relatively higher $\sum_{18}$ PAH C_A in the most northern latitudes of the Arctic Ocean, which is associated with back trajectories of air masses from Sothern Asia. The higher levels of C_A in our study could be attributed to the costal line being close to larger areas of burning taiga forest ~~-~~and more industrial sources in the boreal regions of Russian continent. Similar to the pattern for heavy metals mentioned above, high levels of these chemicals may have been derived from atmospheric transport from the industrial areas of the Russian continent. Because of the ~~different~~ various sampling methods and, ~~different~~ the differences in PAHs measured, ~~total PAH species~~ and because not all ~~reports~~ studies separated gas and particles concentrations, it is quite difficult to compare PAH levels in ~~the~~ aerosols. The average $\sum_{35}$ PAH ~~concentrations in dissolved water (C_W, ng L-1)~~ ranged from 13.07 ng L^{-1} (Laptev Sea) to 69.90 ng L^{-1} (Barents Sea), ~~of which the~~and its spatial variability ~~-~~was similar to that of PAH concentrations in aerosols. The range of $\sum_{35}$ PAH ~~of~~ C_W for the Barents Sea, Kara Sea, Leptev Sea, and East Siberian Sea is 12.36–~~–~~162.05 ng L^{-1}, 12.18–~~–~~14.04 ng L^{-1}, 11.21–~~–~~15.82 ng L^{-1}, and 11.40–~~–~~129.60 ng L^{-1}, respectively. Higher levels of C_W were also found along the coast of the Yamal-Gydan Peninsula, where petrol and natural gas industries have active sites (**Fig. 5c**). ~~The highest $\sum_{35}$ PAH concentration in the gas phase (C_G, ng m^{-3}) occurred in the Barents Sea, and the value was 215 ng m^{-3}. PAH concentrations in aerosols (C_A, ng m^{-3}) in the Barents Sea, Kara Sea, and East Siberian Sea were apparently higher than those in the gas phase (**Fig. 5b**) with average C_A values of 215.67, 130.80, and 77.72 ng m^{-3}, respectively. Similar to the pattern for heavy metals mentioned above, these chemicals may have been derived from atmospheric transport from the Russian continent. The average $\sum_{35}$ PAH concentrations in dissolved water (C_W, ng L^{-1}) ranged from 13.12 ng L^{-1} (Laptev Sea) to 60.88 ng L^{-1} (Barents Sea), of which the variability was similar to that of PAH concentrations in aerosols. Higher levels of C_W were also found along the coast of the Yamal-Gydan Peninsula where petrol and natural gas industries have active sites (**Fig. 5c**).~~

The contribution of each PAH in the gas, aerosol, and dissolved water phases is determined by its source, volatility, and hydrophobicity (Lima et al., 2005). The low-molecular weight PAHs were dominant in gas and dissolved water (**Fig. S5**). In the gas phase, low-~~molecular~~-molecular-weight PAHs occupied more than 75% of the $\sum_{35}$ PAHs, which mainly contained methylated phenanthrenes, e.g., methylphenanthrene (mean = 1.31 ng m^{-3}), dimethylphenanthrene (mean = 1.27 ng m^{-3}), and trimethylphenanthrene (mean = 1.32 ng m^{-3}), and methylated dibenzothiophenes, e.g., methyldibenzothiophene (mean = 1.29 ng m^{-3}), dimethyldibenzothiophene (mean = 1.27 ng m^{-3}), and trimethyldibenzothiophene (mean = 1.32 ng m^{-3}). In dissolved water, methylnapthalene and tetramethylnaphthalene were the most abundant PAHs with average concentrations of 1.12 and 1.45 ng L^{-1}, respectively. Measured values of C_G, C_A, and C_W are known to vary with the changes of

设置了格式: 下标
设置了格式: 下标
设置了格式: 下标
设置了格式: 下标
设置了格式: 下标
设置了格式: 上标
设置了格式: 上标
设置了格式: 下标
设置了格式: 下标
设置了格式: 上标
设置了格式: 上标
设置了格式: 上标
设置了格式: 上标
设置了格式: 下标
设置了格式: 字体: 加粗

each PAH concentration in the marine environment (Berrojalbiz et al., 2011; Castro-Jimenez et al., 2012; Cabrerizo et al., 2014). However, there were no previous reports about the occurrence of PAHs in the Russian Arctic atmosphere and ocean.

The average dry deposition flux (F_{DD}) of the $\sum_{35}$ PAHs was 1108 ng m^{-2} d^{-1}. The increasing values of V_d may influence F_{DD} in the marine environment due to the higher hydrophobicity of organic compounds, surface microlayer with reduced surface tension, and lipid floating (del Vento and Dachs, 2007b). The higher average V_d was observed for 9-methlyfluorene (1.01–10.02 cm s^{-1}), followed by 1,7-dimethylfluorene (1.06–10.63 cm s^{-1}) (**Fig. S6**). On a global scale, higher V_d values were found for heavier PAHs such as methylchrysene (0.17–13.30 cm s^{-1}) and dibenzo(a,h)anthracene (0.29–1.38 cm s^{-1}) (Gonzalez-Gaya et al., 2014). The V_d values reported previously ranged from 0.08 to 0.3 cm s^{-1} in the Atlantic Ocean (Del Vento and Dachs, 2007a) and from 0.01 to 0.8 cm s^{-1} in coastal areas (Holsen and Noll, 1992; Bozlaker et al., 2008; Esen et al., 2008; Eng et al., 2014); the higher values were observed in concentrated industrial and urban areas (Bozlaker et al., 2008). In our study, the highest V_d values were observed in the Barents Sea; the other three seas had similar V_d values ($p > 0.05$) that were lower than in the Barents Sea except for 9-methlyfluorene and 1,7-dimethylfluorene. The East Siberian Sea exhibited the lowest value of V_d, while the relatively higher V_d values were found for heavier PAHs (dibenzo(a,h)anthracene, indeno(1,2,3-cd)pyrene, dibenzo(a,h)anthracene and benzo(g,h,i)perylene) in all seas (**Fig. S7**). This may be due to heavier PAHs being principally deposited via heavier aerosols with a higher V_d because they are bound to hydrophobic aerosols or because of gravity, e.g. soot carbon (Gonzalez-Gaya et al., 2014). Dry deposition is a major process for high-molecular-weight PAHs bound to aerosols (**Fig. 6 and Fig. S8**). The deposition values varied mainly in accordance with the PAH concentrations of aerosols in suspension and the factors influencing the deposition velocities (wind speed, compound vapor pressure, etc.). The F_{WD} of the $\sum_{35}$ PAHs ranged from 14 to 19 μg m^{-2} d^{-1}. Gonzalez-Gaya et al. (2014) found the highest F_{WD} of $\sum_{64}$ PAHs in the North Atlantic Ocean (24 μg m^{-2} d^{-1}) with an average F_{WD} value of ~8 μg m^{-2} d^{-1} on the global scale based on rain samples. The higher F_{WD} values of PAHs were found in urban areas in China (62.6 μg m^{-2} d^{-1}) (Wang et al., 2016) from rain samples and the lower F_{WD} values of PAHs (0.02–0.28 μg m^{-2} d^{-1}) from both rain and snow samples were observed in high mountain European areas (Arellano et al., 2018). Our F_{WD} values were within the range of previously reported global scale and the difference in wet deposition was mainly dependent on source distance and precipitation intensity. Wet deposition is an important purging process for semivolatile organic compounds such as PAHs in the gas and aerosol phase. Snow events are quite sporadic in the Arctic Ocean and thus, these have lower relevance for wet deposition of PAHs in this

设置了格式: 下标

The estimated F_{AW} values revealed that most PAHs had a net input from the atmosphere to the ocean except for the more volatile PAHs, such as 2–3 ring PAHs (**Fig. 7**). The lighter PAHs (2–3 rings) appeared more volatile (978–4892 ng m^{-2} d^{-1}) while heavier PAHs (4–6 rings) showed net deposition (1561–7808 ng m^{-2} d^{-1}), except dibenzo(a,h)anthracene (1322 ng m^{-2} d^{-1}), indeno(1,2,3-cd)pyrene (1238 ng m^{-2} d^{-1}), trimethylphenanthrene (1901 ng m^{-2} d^{-1}) and benzo(g,h,i)perylene (2708 ng m^{-2} d^{-1}). Three orders of magnitude higher net deposition was observed for methylphenanthrene, dimethylphenanthrene, trimethylphenanthrene and tetramethylphenanthrene (**Fig. S9**). Our results were similar to those observed in other PAH-affected areas such as the southeast Mediterranean (Castro-Jimenez et al., 2012), Narragansett Bay (Lohmann et al., 2011) and the North Atlantic Ocean (Lohmann et al., 2009). Ma et al. (2013) suggested that slight volatilization of lighter PAHs may exist from additional sources such as ship ballast and riverine runoff, which is consistent with our findings that volatilization occurred mainly in the East Siberian Sea and Barents Sea, where more industrial factories and urban areas are situated. Our study is also consistent with previous reports showing that diffusion during air–water exchange is the main process for transfer of relatively light volatile organic compounds to the marine environment (Castro-Jimenez et al., 2012; Jurado et al., 2005). ~~The estimated net diffusion of air–water exchange (F_{AW}, ng m^{-2} d^{-1}) revealed that most PAHs had net inputs from the atmosphere to ocean except for the more volatile PAHs such as 2–3 ring PAHs (**Fig. 6b**). This is consistent with previous reports in which the results showed that diffusion during air–water exchange is the main process for transfers of relatively lighter volatile organic compounds in the marine environment (Castro-Jimenez et al., 2012; Jurado et al., 2005).~~ The integrated monthly F_{AW} ~~fluxes~~ (tons~~nes~~ per month) of 5–6 ring PAHs were comparable to F_{DD} ~~fluxes~~ values in the Russian Arctic Ocean, whereas only the East Siberian Sea showed high~~er~~ levels of dry deposition (**Fig. ~~S6~~S9**). In all ~~of the~~ four seas, ~~the~~ F_{AW} ~~fluxes~~ values of 3–4 ring PAHs were ~~at~~ of the same magnitude as ~~the~~ F_{DD} ~~fluxes~~values. The total volatilization and total adsorption of the $\sum_{35}$ PAHs in the Russian Arctic Ocean amounted to 2600 ton~~ne~~s per month and 3640 ton~~ne~~s per month, respectively~~.~~, Therefore~~and thus~~, there was a net input of the $\sum_{35}$ PAHs from the atmosphere to the marine environment that reached 3276 ton~~ne~~s, which was 100 times higher than for the aerosol-bound $\sum_{35}$ PAHs that underwent dry deposition (estimated at ~~around~~ ~30 tons~~nes~~ per month). In other reports, Gonzalez-Gaya et al. (2016) estimated the global input of PAHs from the atmosphere to the ocean to be on the order of 90,000 ton~~ne~~s per month and Reddy et al. (2012) reported that the input of PAHs to the ocean in the Gulf of Mexico in 2010 after the ~~enormous~~ Deepwater Horizon oil spill was 20,000 ton~~ne~~s. Such comparisons suggest that the diffusive fluxes in the Russian Arctic Ocean play an

important role in the atmosphere–ocean exchange of PAHs, whereas there is a ~~relatively~~ lower input of PAHs to the Russian Arctic Ocean on the global scale.

In addition to the transfers of PAHs to the ocean, PAHs also can be degraded during transport through the atmosphere because of reactions with OH radicals (Keyte et al., 2013). The degradation flux~~es (~~ (D_{atm}~~, ng m^{-2} d^{-1})~~ of PAHs in the gas phase of the oceanic atmosphere (**Fig. ~~7~~8**) was estimated at 3000 ton~~ne~~s per month for the $\sum_{35}$ PAHs, ~~and this~~which represents an additional PAH sink (see Methods). In general, the large amounts of PAHs undergoing net deposition to the ocean and degradation during atmospheric transport ~~must be~~are indicative of large source areas in the Russian Arctic. Notably, PAHs concentrations have been increasing in the atmosphere owing to wildfires and fossil fuel use over the past century (Zhang and Tao, 2009). The high-molecular weight PAHs were dominant in the aerosols (**Fig. 5**) originating from pyrolytic sources (Lima et al., 2005). Besides, high abundances of alkylated PAHs were observed in the gas and dissolved phases, and along with the evaluations of the diagnostic ratios (**Fig. ~~S7~~S10**), the results were suggestive of pyrogenic sources for PAHs in gases and aerosols, and mixtures of pyrogenic and petrogenic sources for PAHs in dissolved water (mostly for the Leptev Sea and East Siberian Sea). Other sources contributing to the occurrence of PAHs may have involved both anthropogenic and biogenic sources on ~~the~~ land (Cabrerizo et al., 2011). In ~~this region~~the Russian Arctic Ocean, it can be assumed that PAHs in the atmosphere (gas and aerosol) originated from anthropogenic sources including industrial and urban activities, while PAHs in ~~the~~ seawater, at ~~the~~ sites with relatively less anthropogenic sources, i.e., the Leptev Sea and East Siberian Sea, originated from a mixture of anthropogenic and biogenic sources. This indicates that atmospheric transport of PAHs derived from anthropogenic activities occurs in all sectors of the Russian Arctic Ocean while only the East Siberian Sea and Leptev Sea have more anthropogenic PAHs in the water phase.~~This indicates that atmospheric transport of PAHs derived from anthropogenic activities is the main input pathway for the Arctic Ocean.~~

Because PAHs are toxic, these chemicals can have an adverse influence on food webs in marine ecosystems (Hylland, 2006). In particular, even though PAHs are present at natural background levels in the marine environment, the massive usage of fossil fuels has led to increases in PAH emissions and excessive PAH concentrations in many marine environments. The present study indicates that there are high contributions of diffusive atmospheric PAHs to the Arctic Ocean, and these chemicals are potentially perturbing the carbon cycle in the ocean and posing risks to the fragile Arctic marine food webs. Thus, further studies of the impacts of such chemicals are warranted.

4 Conclusion

This study presents the occurrence and atmosphere–ocean fluxes of 35 PAHs and 9 heavy metals in the Arctic Ocean. Dry deposition and wet deposition fluxes of ~~nine~~ 9 heavy metals in aerosols were estimated at 2205 ng m^{-2} d^{-1} and 10.95 μg m^{-2} d^{-1}, respectively. The net gross absorption of Hg in the Arctic Ocean was estimated at 280 ton~~ne~~s per month. A net input of PAHs from the atmosphere to the Arctic Ocean was observed for most of the PAHs ~~(35 species)~~, especially for the low-molecular weight PAHs. The net atmospheric input of the 35 PAHs was estimated at 3276 ton~~ne~~s per month. The current occurrences of semivolatile aromatic hydrocarbons could have been derived from biogenic sources and anthropogenic sources from continental land masses, especially for the locations close to industrial areas. These input<u>s</u> ~~concentrations~~ of Hg and PAHs ~~sources~~ may be causing adverse effects on the fragile Arctic marine ecosystems~~, and~~<u>;</u> this issue warrants further research. <u>In addition, our study suggests that both PAHs and metals are affected by local depositional effects and change of source emission, and therefore, spatial distribution of these compounds and source identification need to be further investigated.</u>

Author contributions. Dr. Xiaowen Ji and Dr. Evgeny Abakumov set up the sampling equipment and ~~measured~~ <u>analyzed</u> the samples, and ~~they analyzed~~ the data. Dr. Xianchuan Xie also helped to collect and analyze the data. Dr. Xiaowen Ji and Dr. Xianchuan Xie wrote this manuscript.

Competing interests. The authors declare that they have no conflict of interest.

Acknowledgements. This work was supported by grants from the Russian Foundation for Basic Research (18-44-890003, 16-34-60010); by a grant from Saint-Petersburg State University titled “Urbanized ecosystems of the Russian Arctic: dynamics, state and sustainable development”; by the Jiangsu Nature Science Fund (BK20151378), and by the Fundamental Research Funds for the Central Universities (090514380001)<u>. ~~.~~We would like to thank Miss Yu Su from the School of Visual Art, BFA Computer Art for helping to draw supplementary journal cover, and Miss Kuznetsova Ekaterina for helping with the Russian translation.</u>

References

Andersson, M. E., Gårdfeldt, K., Wängberg, I., and Strömberg, D.: Determination of Henry's law constant for elemental mercury, Chemosphere, 73, 587-592, 10.1016/j.chemosphere.2008.05.067, 2008.

Arellano, L., Fernández, P., van Drooge, B. L., Rose, N. L., Nickus, U., Thies, H., Stuchlík, E., Camarero, L., Catalan, J., and Grimalt, J. O.: Drivers of atmospheric deposition of polycyclic aromatic hydrocarbons at European high-altitude sites, Atmos. Chem. Phys., 18, 16081-16097, 10.5194/acp-18-16081-2018, 2018.

Ariya, P. A., Dastroor, A. P., Amyot, M., Schroeder, W. H., Barrie, L., Anlauf, K., Raofie, F., Ryzhkov, A., Davignon, D., Lalonde, J., and Steffen, A.: The Arctic: a sink for mercury, Tellus B: Chemical and Physical Meteorology, 56, 397-403, 10.3402/tellusb.v56i5.16458, 2004.

Bagi, A., Pampanin, D. M., Lanzén, A., Bilstad, T., and Kommedal, R.: Naphthalene biodegradation in temperate and arctic marine microcosms, Biodegradation, 25, 111-125, 10.1007/s10532-013-9644-3, 2014.

Bamford, H. A., Poster, D. L., and Baker, J. E.: Temperature dependence of Henry's law constants of thirteen polycyclic aromatic hydrocarbons between 4 degrees C and 31 degrees C, Environ. Toxicol. Chem., 18, 1905-1912, 10.1897/1551-5028(1999)018<1905:Tdohsl>2.3.Co;2, 1999.

Berrojalbiz, N., Dachs, J., Jose Ojeda, M., Carmen Valle, M., Castro-Jimenez, J., Wollgast, J., Ghiani, M., Hanke, G., and Zaldivar, J. M.: Biogeochemical and physical controls on concentrations of polycyclic aromatic hydrocarbons in water and plankton of the Mediterranean and Black Seas, Global Biogeochem. Cycles, 25, 10.1029/2010gb003775, 2011.

Bigg, E. K., and Leck, C.: Properties of the aerosol over the central Arctic Ocean, Journal of Geophysical Research: Atmospheres, 106, 32101-32109, 10.1029/1999JD901136, 2001.

Boyd, R., Barnes, S. J., De Caritat, P., Chekushin, V. A., Melezhik, V. A., Reimann, C., and Zientek, M. L.: Emissions from the copper-nickel industry on the Kola Peninsula and at Noril'sk, Russia, Atmos. Environ., 43, 1474-1480, 10.1016/j.atmosenv.2008.12.003, 2009.

Bozlaker, A., Muezzinoglu, A., and Odabasi, M.: Atmospheric concentrations, dry deposition and air-soil exchange of polycyclic aromatic hydrocarbons (PAHs) in an industrial region in Turkey, J. Hazard. Mater., 153, 1093-1102, 10.1016/j.jhazmat.2007.09.064, 2008.

Brooks, S. B., Saiz-Lopez, A., Skov, H., Lindberg, S. E., Plane, J. M. C., and Goodsite, M. E.: The mass balance of mercury in the springtime arctic environment, Geophysical Research Letters, 33, 10.1029/2005GL025525, 2006.

Burkhard, L. P.: Estimating dissolved organic carbon partition coefficients for nonionic organic chemicals, Environmental Science & Technology, 34, 4663-4668, 10.1021/es001269I, 2000.

Cabrerizo, A., Dachs, J., Moeckel, C., Ojeda, M.-J., Caballero, G., Barcelo, D., and Jones, K. C.: Ubiquitous Net Volatilization of Polycyclic Aromatic Hydrocarbons from Soils and Parameters Influencing Their Soil-Air Partitioning, Environmental Science & Technology, 45, 4740-4747, 10.1021/es104131f, 2011.

Cabrerizo, A., Galban-Malagon, C., Del Vento, S., and Dachs, J.: Sources and fate of polycyclic aromatic hydrocarbons in the Antarctic and Southern Ocean atmosphere, Global Biogeochem. Cycles, 28, 1424-1436, 10.1002/2014gb004910, 2014.

Castro-Jimenez, J., Berrojalbiz, N., Wollgast, J., and Dachs, J.: Polycyclic aromatic hydrocarbons (PAHs) in the Mediterranean Sea: Atmospheric occurrence, deposition and decoupling with settling fluxes in the water column, Environ. Pollut., 166, 40-47, 10.1016/j.envpol.2012.03.003, 2012.

Chen, Y., Paytan, A., Chase, Z., Measures, C., Beck, A. J., Sañudo-Wilhelmy, S. A., and Post, A. F.: Sources and fluxes of atmospheric trace elements to the Gulf of Aqaba, Red Sea, Journal of Geophysical Research: Atmospheres, 113, 10.1029/2007JD009110, 2008.

Cheng, J.-O., Ko, F.-C., Lee, C.-L., and Fang, M.-D.: Air–water exchange fluxes of polycyclic aromatic hydrocarbons in the tropical coast, Taiwan, Chemosphere, 90, 2614-2622, 10.1016/j.chemosphere.2012.11.020, 2013.

Cheng, M. D., Hopke, P. K., Barrie, L., Rippe, A., Olson, M., and Landsberger, S.: Qualitative determination of source regions of aerosol in Canadian high Arctic, Environmental Science & Technology, 27, 2063-2071, 10.1021/es00047a011, 1993.

Chester, R., Nimmo, M., and Preston, M. R.: The trace metal chemistry of atmospheric dry deposition samples collected at Cap Ferrat: a coastal site in the Western Mediterranean, Mar. Chem., 68, 15-30, doi.org/10.1016/S0304-4203(99)00062-6, 1999.

Cone, M.: Silent Snow: The Slow Poisoning of the Arctic, Paw Prints, 2008.

Custódio, D., Cerqueira, M., Fialho, P., Nunes, T., Pio, C., and Henriques, D.: Wet deposition of particulate carbon to the Central North Atlantic Ocean, Sci. Total Environ., 496, 92-99, 10.1016/j.scitotenv.2014.06.103, 2014.

Dahle, S., Savinov, V., Carroll, J., Vladimirov, M., Ivanov, G., Valetova, N., Gaziev, Y., Dunaev, G., Kirichenko, Z., Nikitin, A., Petrenko, G., Polukhina, A., Kalmykov, S., Aliev, R., and Sabodina, M.: A return to the nuclear waste dumping sites in the Bays of Novaya Zemlya, 2009.

Del Vento, S., and Dachs, J.: Atmospheric occurrence and deposition of polycyclic aromatic hydrocarbons in the northeast tropical and subtropical Atlantic Ocean, Environmental Science & Technology, 41, 5608-5613, 10.1021/es0707660, 2007a.

del Vento, S., and Dachs, J.: Influence of the surface microlayer on atmospheric deposition of aerosols and polycyclic aromatic hydrocarbons, Atmos. Environ., 41, 4920-4930, 10.1016/j.atmosenv.2007.01.062, 2007b.

Duce, R. A., Liss, P. S., Merrill, J. T., Atlas, E. L., Buat-Menard, P., Hicks, B. B., Miller, J. M., Prospero, J. M., Arimoto, R., Church, T. M., Ellis, W., Galloway, J. N., Hansen, L., Jickells, T. D., Knap, A. H.,

Reinhardt, K. H., Schneider, B., Soudine, A., Tokos, J. J., Tsunogai, S., Wollast, R., and Zhou, M.: The atmospheric input of trace species to the world ocean, Global Biogeochem. Cycles, 5, 193-259, 10.1029/91GB01778, 1991.

Eng, A., Harner, T., and Pozo, K.: A Prototype Passive Air Sampler for Measuring Dry Deposition of Polycyclic Aromatic Hydrocarbons, Environmental Science & Technology Letters, 1, 77-81, 10.1021/ez400044z, 2014.

Environment-Canada;, Oceans-Canada;, F., and Affairs-Canada;, I. a. N.: Land-Based Pollution in the Arctic Ocean: Canadian Actions in a Regional and Global Context, Arctic, 61, 111-121, 2008.

Esen, F., Cindoruk, S. S., and Tasdemir, Y.: Bulk deposition of polycyclic aromatic hydrocarbons (PAHs) in an industrial site of Turkey, Environ. Pollut., 152, 461-467, 10.1016/j.envpol.2007.05.031, 2008.

Fernandes, M. B., and Sicre, M. A.: Polycyclic Aromatic Hydrocarbons in the Arctic: Ob and Yenisei Estuaries and Kara Sea Shelf, Estuarine, Coastal and Shelf Science, 48, 725-737, https://doi.org/10.1006/ecss.1999.0472, 1999.

Ferrero, L., Sangiorgi, G., Perrone, M. G., Rizzi, C., Cataldi, M., Markuszewski, P., Pakszys, P., Makuch, P., Petelski, T., Becagli, S., Traversi, R., Bolzacchini, E., and Zielinski, T.: Chemical Composition of Aerosol over the Arctic Ocean from Summer ARctic EXpedition (AREX) 2011–2012 Cruises: Ions, Amines, Elemental Carbon, Organic Matter, Polycyclic Aromatic Hydrocarbons, n-Alkanes, Metals, and Rare Earth Elements, Atmosphere, 10, 54, 2019.

Galarneau, E., Patel, M., Brook, J. R., Charland, J.-P., Glasius, M., Bossi, R., and Hung, H.: Artefacts in semivolatile organic compound sampling with polyurethane foam substrates in high volume cascade impactors, Aerosol Sci. Technol., 51, 247-257, 10.1080/02786826.2016.1267327, 2017.

Gonzalez-Gaya, B., Zuniga-Rival, J., Ojeda, M.-J., Jimenez, B., and Dachs, J.: Field Measurements of the Atmospheric Dry Deposition Fluxes and Velocities of Polycyclic Aromatic Hydrocarbons to the Global Oceans, Environmental Science & Technology, 48, 5583-5592, 10.1021/es500846p, 2014.

Gonzalez-Gaya, B., Fernandez-Pinos, M.-C., Morales, L., Mejanelle, L., Abad, E., Pina, B., Duarte, C. M., Jimenez, B., and Dachs, J.: High atmosphere-ocean exchange of semivolatile aromatic hydrocarbons, Nature Geoscience, 9, 438-+, 10.1038/ngeo2714, 2016.

Grosjean, D.: Polycyclic aromatic hydrocarbons in Los Angeles air from samples collected on teflon, glass and quartz filters, Atmospheric Environment (1967), 17, 2565-2573, https://doi.org/10.1016/0004-6981(83)90084-7, 1983.

Harris, R. C., Rudd, J. W. M., Amyot, M., Babiarz, C. L., Beaty, K. G., Blanchfield, P. J., Bodaly, R. A., Branfireun, B. A., Gilmour, C. C., Graydon, J. A., Heyes, A., Hintelmann, H., Hurley, J. P., Kelly, C. A., Krabbenhoft, D. P., Lindberg, S. E., Mason, R. P., Paterson, M. J., Podemski, C. L., Robinson, A., Sandilands, K. A., Southworth, G. R., St. Louis, V. L., and Tate, M. T.: Whole-ecosystem study shows rapid fish-mercury response to changes in mercury deposition, Proceedings of the National Academy of Sciences, 104, 16586, 10.1073/pnas.0704186104, 2007.

Holsen, T. M., and Noll, K. E.: Dry deposition of atmospheric particles - application of current models to ambient data, Environmental Science & Technology, 26, 1807-1815, 10.1021/es00033a015, 1992.

Hornbuckle, K. C., Jeremiason, J. D., Sweet, C. W., and Eisenreich, S. J.: Seasonal Variations in Air-Water Exchange of Polychlorinated Biphenyls in Lake Superior, Environmental Science & Technology, 28, 1491-1501, 10.1021/es00057a018, 1994.

Hung, H., Katsoyiannis, A. A., Brorström-Lundén, E., Olafsdottir, K., Aas, W., Breivik, K., Bohlin-Nizzetto, P., Sigurdsson, A., Hakola, H., Bossi, R., Skov, H., Sverko, E., Barresi, E., Fellin, P., and Wilson, S.: Temporal trends of Persistent Organic Pollutants (POPs) in arctic air: 20 years of monitoring under the Arctic Monitoring and Assessment Programme (AMAP), Environ. Pollut., 217, 52-61, https://doi.org/10.1016/j.envpol.2016.01.079, 2016.

Hylland, K.: Polycyclic Aromatic Hydrocarbon (PAH) Ecotoxicology in Marine Ecosystems, Journal of Toxicology and Environmental Health, Part A, 69, 109-123, 10.1080/15287390500259327, 2006.

Jaffe, D., Cerundolo, B., Rickers, J., Stolzberg, R., and Baklanov, A.: Deposition of sulfate and heavy-metals on the Kola-Peninsula, Sci. Total Environ., 160-61, 127-134, 10.1016/0048-9697(95)04350-a, 1995.

Ji, X., Abakumov, E., and Polyakov, V.: Assessments of pollution status and human health risk of heavy metals in permafrost-affected soils and lichens: A case-study in Yamal Peninsula, Russia Arctic AU - Ji, Xiaowen, Human and Ecological Risk Assessment: An International Journal, 1-18, 10.1080/10807039.2018.1490887, 2019.

Jickells, T. D., and Baker, A. R.: Atmospheric Transport and Deposition of Particulate Matter to the Oceans, in: Encyclopedia of Ocean Sciences (Third Edition), edited by: Cochran, J. K., Bokuniewicz, H. J., and Yager, P. L., Academic Press, Oxford, 21-25, 2019.

Jurado, E., Jaward, F., Lohmarm, R., Jones, K. C., Simo, R., and Dachs, J.: Wet deposition of persistent organic pollutants to the global oceans (vol 39, pg 2426, 2005), Environmental Science & Technology, 39, 4672-4672, 10.1021/es050660+, 2005.

Keyte, I. J., Harrison, R. M., and Lammel, G.: Chemical reactivity and long-range transport potential of polycyclic aromatic hydrocarbons – a review, Chem. Soc. Rev., 42, 9333-9391, 10.1039/C3CS60147A, 2013.

Kim, K.-H., Ebinghaus, R., Schroeder, W. H., Blanchard, P., Kock, H. H., Steffen, A., Froude, F. A., Kim, M.-Y., Hong, S., and Kim, J.-H.: Atmospheric Mercury Concentrations from Several Observatory Sites in the Northern Hemisphere, Journal of Atmospheric Chemistry, 50, 1-24, 10.1007/s10874-005-9222-0, 2005.

Kondo, Y., Obata, H., Hioki, N., Ooki, A., Nishino, S., Kikuchi, T., and Kuma, K.: Transport of trace metals (Mn, Fe, Ni, Zn and Cd) in the western Arctic Ocean (Chukchi Sea and Canada Basin) in late summer 2012, Deep Sea Research Part I: Oceanographic Research Papers, 116, 236-252, https://doi.org/10.1016/j.dsr.2016.08.010, 2016.

Leck, C., Bigg, E. K., Covert, D. S., Heintzenberg, J., Maenhaut, W., Nilsson, E. D., and Wiedensohler, A.: Overview of the atmospheric research program during the International Arctic Ocean Expedition of 1991 (IAOE-91) and its scientific results, Tellus B, 48, 136-155, 10.1034/j.1600-0889.1996.t01-1-00002.x, 1996.

Lima, A. L. C., Farrington, J. W., and Reddy, C. M.: Combustion-Derived Polycyclic Aromatic Hydrocarbons in the Environment—A Review, Environmental Forensics, 6, 109-131, 10.1080/15275920590952739, 2005.

Lindberg, S. E., Brooks, S., Lin, C. J., Scott, K., Meyers, T., Chambers, L., Landis, M., and Stevens, R.: Formation of Reactive Gaseous Mercury in the Arctic: Evidence of Oxidation of Hg° to Gas-Phase Hg-II Compounds after Arctic Sunrise, Water, Air and Soil Pollution: Focus, 1, 295-302, 10.1023/A:1013171509022, 2001.

Livingstone, D. M., and Imboden, D. M.: The nonlinear influence of wind-speed variability on gas transfer in lakes Tellus Series B-Chemical and Physical Meteorology, 45, 275-295, 10.1034/j.1600-0889.1993.t01-2-00005.x, 1993.

Lohmann, R., Gioia, R., Jones, K. C., Nizzetto, L., Temme, C., Xie, Z., Schulz-Bull, D., Hand, I., Morgan, E., and Jantunen, L.: Organochlorine Pesticides and PAHs in the Surface Water and Atmosphere of the North Atlantic and Arctic Ocean, Environmental Science & Technology, 43, 5633-5639, 10.1021/es901229k, 2009.

Lohmann, R., Dapsis, M., Morgan, E. J., Dekany, V., and Luey, P. J.: Determining Air−Water Exchange, Spatial and Temporal Trends of Freely Dissolved PAHs in an Urban Estuary Using Passive Polyethylene Samplers, Environmental Science & Technology, 45, 2655-2662, 10.1021/es1025883, 2011.

Ma, Y., Xie, Z., Yang, H., Möller, A., Halsall, C., Cai, M., Sturm, R., and Ebinghaus, R.: Deposition of polycyclic aromatic hydrocarbons in the North Pacific and the Arctic, Journal of Geophysical Research: Atmospheres, 118, 5822-5829, 10.1002/jgrd.50473, 2013.

Maenhaut, W., Zoller, W. H., Duce, R. A., and Hoffman, G. L.: Concentration and size distribution of particulate trace elements in the south polar atmosphere, Journal of Geophysical Research: Oceans, 84, 2421-2431, 10.1029/JC084iC05p02421, 1979.

Maenhaut, W., Cornille, P., Pacyna, J. M., and Vitols, V.: Trace element composition and origin of the atmospheric aerosol in the Norwegian arctic, Atmospheric Environment (1967), 23, 2551-2569, 10.1016/0004-6981(89)90266-7, 1989.

Maenhaut, W., Ducastel, G., Leck, C., Nilsson, E., and Heintzenberg, J.: Multi-elemental composition and sources of the high Arctic atmospheric aerosol during summer and autumn, Tellus B, 48, 300-321, 10.1034/j.1600-0889.1996.t01-1-00011.x, 2002.

Mariraj Mohan, S.: An overview of particulate dry deposition: measuring methods, deposition velocity and controlling factors, International Journal of Environmental Science and Technology, 13, 387-402, 10.1007/s13762-015-0898-7, 2016.

Mason, R. P., and Sheu, G.-R.: Role of the ocean in the global mercury cycle, Global Biogeochem. Cycles, 16, 40-41-40-14, 10.1029/2001GB001440, 2002.

Nightingale, P. D., Liss, P. S., and Schlosser, P.: Measurements of air-sea gas transfer during an open ocean algal bloom, Geophysical Research Letters, 27, 2117-2120, 10.1029/2000gl011541, 2000.

Pacyna, E. G., Pacyna, J. M., Sundseth, K., Munthe, J., Kindbom, K., Wilson, S., Steenhuisen, F., and Maxson, P.: Global emission of mercury to the atmosphere from anthropogenic sources in 2005 and projections to 2020, Atmos. Environ., 44, 2487-2499, 10.1016/j.atmosenv.2009.06.009, 2010.

Park, G.-H., Lee, S.-E., Kim, Y.-i., Kim, D., Lee, K., Kang, J., Kim, Y.-H., Kim, H., Park, S., and Kim, T.-W.: Atmospheric deposition of anthropogenic inorganic nitrogen in airborne particles and precipitation in the East Sea in the northwestern Pacific Ocean, Sci. Total Environ., 681, 400-412, 10.1016/j.scitotenv.2019.05.135, 2019.

Pearson, C., Howard, D., Moore, C., and Obrist, D.: Mercury and trace metal wet deposition across five stations in Alaska: controlling factors, spatial patterns, and source regions, Atmos. Chem. Phys., 19, 6913-6929, 10.5194/acp-19-6913-2019, 2019.

Peters, K., and Eiden, R.: Modelling the dry deposition velocity of aerosol particles to a spruce forest, Atmospheric Environment. Part A. General Topics, 26, 2555-2564, 10.1016/0960-1686(92)90108-W, 1992.

Poissant, L., Zhang, H. H., Canário, J., and Constant, P.: Critical review of mercury fates and contamination in the arctic tundra ecosystem, Sci. Total Environ., 400, 173-211, 10.1016/j.scitotenv.2008.06.050, 2008.

Rahn, K. A., and Lowenthal, D. H.: Elemental traces of distant regional pollution aerosols Science, 223, 132-139, 10.1126/science.223.4632.132, 1984.

Rasiq, K. T., El-Maradny, A., Orif, M., Bashir, M. E., and Turki, A. J.: Polycyclic aromatic hydrocarbons in two polluted lagoons, eastern coast of the Red Sea: Levels, probable sources, dry deposition fluxes and air-water exchange, Atmospheric Pollution Research, 10, 880-888, doi.org/10.1016/j.apr.2018.12.016, 2019.

Rasmussen, R., Baker, B., Kochendorfer, J., Myers, T., Landolt, S., Fischer, A., Black, J., Thériault, J., Kucera, P., Gochis, D., Smith, C., Nitu, R., Hall, M., Cristanelli, S., and Gutmann, A.: How well are we measuring snow: the NOAA/FAA/NCAR winter precipitation test bed, 2012.

Reddy, C. M., Arey, J. S., Seewald, J. S., Sylva, S. P., Lemkau, K. L., Nelson, R. K., Carmichael, C. A., McIntyre, C. P., Fenwick, J., Ventura, G. T., Van Mooy, B. A. S., and Camilli, R.: Composition and fate of gas and oil released to the water column during the Deepwater Horizon oil spill, Proceedings of the National Academy of Sciences of the United States of America, 109, 20229-20234, 10.1073/pnas.1101242108, 2012.

Reimann, C., Boyd, R., deCaritat, P., Halleraker, J. H., Kashulina, G., Niskavaara, H., and Bogatyrev, I.: Topsoil (0-5 cm) composition in eight arctic catchments in northern Europe (Finland, Norway and Russia), Environ. Pollut., 95, 45-56, 10.1016/s0269-7491(96)00102-9, 1997.

Robert, P. M.: Trace Metals in Freshwaters, in: Trace Metals in Aquatic Systems, 2013.

Rovinsky, F., Pastukhov, B., Bouyvolov, Y., and Burtseva, L.: Present day state of background pollution of the natural environment in the Russian Arctic in the region of the Ust-Lena Reserve, Sci. Total Environ., 160-161, 193-199, 10.1016/0048-9697(95)04356-6, 1995.

Selin, N. E., Jacob, D. J., Park, R. J., Yantosca, R. M., Strode, S., Jaeglé, L., and Jaffe, D.: Chemical cycling and deposition of atmospheric mercury: Global constraints from observations, Journal of Geophysical Research: Atmospheres, 112, 10.1029/2006JD007450, 2007.

Shaw, G. E.: Aerosol chemical components in Alaska air masses 1. Aged pollution, Journal of Geophysical Research-Atmospheres, 96, 22357-22368, 10.1029/91jd02058, 1991.

Shevchenko, V., Lisitzin, A., Vinogradova, A., and Stein, R.: Heavy metals in aerosols over the seas of the Russian Arctic, Sci. Total Environ., 306, 11-25, 10.1016/S0048-9697(02)00481-3, 2003.

Shevchenko, V. P., Lisitzin, A. P., Stein, R., Serova, V. V., Isaeva, A. B., and Politova, N. V.: The Composition of the Coarse Fraction of Aerosols in the Marine Boundary Layer over the Laptev, Kara and Barents Seas, in: Land-Ocean Systems in the Siberian Arctic: Dynamics and History, edited by: Kassens, H., Bauch, H. A., Dmitrenko, I. A., Eicken, H., Hubberten, H.-W., Melles, M., Thiede, J., and Timokhov, L. A., Springer Berlin Heidelberg, Berlin, Heidelberg, 53-58, 1999.

Shoeib, M., and Harner, T.: Characterization and Comparison of Three Passive Air Samplers for Persistent Organic Pollutants, Environmental Science & Technology, 36, 4142-4151, 10.1021/es020635t, 2002.

Singh, V. P., and Xu, C. Y.: Evaluation and generalization of 13 mass-transfer equations for determining free water evaporation, Hydrological Processes, 11, 311-323, 10.1002/(SICI)1099-1085(19970315)11:3<311::AID-HYP446>3.0.CO;2-Y, 1997.

Sirois, A., and Barrie, L. A.: Arctic lower tropospheric aerosol trends and composition at Alert, Canada: 1980–1995, Journal of Geophysical Research: Atmospheres, 104, 11599-11618, 10.1029/1999JD900077, 1999.

Skov, H., Brooks, S. B., Goodsite, M. E., Lindberg, S. E., Meyers, T. P., Landis, M. S., Larsen, M. R. B., Jensen, B., McConville, G., and Christensen, J.: Fluxes of reactive gaseous mercury measured with a newly

developed method using relaxed eddy accumulation, Atmos. Environ., 40, 5452-5463, 10.1016/j.atmosenv.2006.04.061, 2006.

Slemr, F., Brunke, E.-G., Ebinghaus, R., Temme, C., Munthe, J., Wängberg, I., Schroeder, W., Steffen, A., and Berg, T.: Worldwide trend of atmospheric mercury since 1977, Geophysical Research Letters, 30, 10.1029/2003GL016954, 2003.

Spivakovsky, C. M., Logan, J. A., Montzka, S. A., Balkanski, Y. J., Foreman-Fowler, M., Jones, D. B. A., Horowitz, L. W., Fusco, A. C., Brenninkmeijer, C. A. M., Prather, M. J., Wofsy, S. C., and McElroy, M. B.: Three-dimensional climatological distribution of tropospheric OH: Update and evaluation, Journal of Geophysical Research-Atmospheres, 105, 8931-8980, 10.1029/1999jd901006, 2000.

Steffen, A., Schroeder, W., Bottenheim, J., Narayan, J., and Fuentes, J. D.: Atmospheric mercury concentrations: measurements and profiles near snow and ice surfaces in the Canadian Arctic during Alert 2000, Atmos. Environ., 36, 2653-2661, 10.1016/S1352-2310(02)00112-7, 2002.

Steffen, A., Schroeder, W., Macdonald, R., Poissant, L., and Konoplev, A.: Mercury in the Arctic atmosphere: An analysis of eight years of measurements of GEM at Alert (Canada) and a comparison with observations at Amderma (Russia) and Kuujjuarapik (Canada), Sci. Total Environ., 342, 185-198, 10.1016/j.scitotenv.2004.12.048, 2005.

Stow, J., Krümmel, E., Leech, T., Donaldson, S., Hansen, J. C., and Van Oostdam, J.: What is the impact of mercury contamination on human health in the Arctic?, AMAP Assessment 2011: Mercury in the Arctic, 159-169, 2015.

Strode, S. A., Jaeglé, L., Selin, N. E., Jacob, D. J., Park, R. J., Yantosca, R. M., Mason, R. P., and Slemr, F.: Air-sea exchange in the global mercury cycle, Global Biogeochem. Cycles, 21, 10.1029/2006GB002766, 2007.

Sunderland, E. M., and Mason, R. P.: Human impacts on open ocean mercury concentrations, Global Biogeochem. Cycles, 21, 10.1029/2006GB002876, 2007.

Totten, L. A., Brunciak, P. A., Gigliotti, C. L., Dachs, J., Glenn, Nelson, E. D., and Eisenreich, S. J.: Dynamic Air−Water Exchange of Polychlorinated Biphenyls in the New York−New Jersey Harbor Estuary, Environmental Science & Technology, 35, 3834-3840, 10.1021/es010791k, 2001.

Vieira, L. H., Achterberg, E. P., Scholten, J., Beck, A. J., Liebetrau, V., Mills, M. M., and Arrigo, K. R.: Benthic fluxes of trace metals in the Chukchi Sea and their transport into the Arctic Ocean, Mar. Chem., 208, 43-55, 10.1016/j.marchem.2018.11.001, 2019.

Vihma, T., Jaagus, J., Jakobson, E., and Palo, T.: Meteorological conditions in the Arctic Ocean in spring and summer 2007 as recorded on the drifting ice station Tara, Geophysical Research Letters, 35, 10.1029/2008GL034681, 2008.

Vinogradova, A., and Polissar, A.: Elemental composition of the aerosol in the atmosphere of the central Russian Arctic **(in Russian)**, Izv Atmos Oceanic Phys, 248-257 pp., 1995.

Vinogradova, A. A., and Ivanova, Y. A.: Heavy Metals in the Atmosphere over the Northern Coast of Eurasia: Interannual Variations in Winter and Summer, Izvestiya, Atmospheric and Oceanic Physics, 53, 711-718, 10.1134/S000143381707009X, 2017.

Walker, T. R., Young, S. D., Crittenden, P. D., and Zhang, H.: Anthropogenic metal enrichment of snow and soil in north-eastern European Russia, Environ. Pollut., 121, 11-21, 10.1016/s0269-7491(02)00212-9, 2003.

Wang, F., Feng, T., Guo, Z., Li, Y., Lin, T., and Rose, N. L.: Sources and dry deposition of carbonaceous aerosols over the coastal East China Sea: Implications for anthropogenic pollutant pathways and deposition, Environ. Pollut., 245, 771-779, doi.org/10.1016/j.envpol.2018.11.059, 2019.

Wang, Q., Liu, M., Li, Y., Liu, Y., Li, S., and Ge, R.: Dry and wet deposition of polycyclic aromatic hydrocarbons and comparison with typical media in urban system of Shanghai, China, Atmos. Environ., 144, 175-181, https://doi.org/10.1016/j.atmosenv.2016.08.079, 2016.

Wängberg, I., Munthe, J., Berg, T., Ebinghaus, R., Kock, H. H., Temme, C., Bieber, E., Spain, T. G., and Stolk, A.: Trends in air concentration and deposition of mercury in the coastal environment of the North Sea Area, Atmos. Environ., 41, 2612-2619, 10.1016/j.atmosenv.2006.11.024, 2007.

Wong, C. S. C., Duzgoren-Aydin, N. S., Aydin, A., and Wong, M. H.: Sources and trends of environmental mercury emissions in Asia, Sci. Total Environ., 368, 649-662, doi.org/10.1016/j.scitotenv.2005.11.024, 2006.

Wu, S.: Polycyclic Aromatic Hydrocarbons in the Atmosphere of Two Subtropical Cities in Southeast China: Seasonal Variation and Gas/Particle Partitioning, Aerosol and Air Quality Research, 10.4209/aaqr.2013.01.0015, 2014.

Zhang, L., Gong, S., Padro, J., and Barrie, L.: A size-segregated particle dry deposition scheme for an atmospheric aerosol module, Atmos. Environ., 35, 549-560, 10.1016/S1352-2310(00)00326-5, 2001.

Zhang, Y., and Tao, S.: Global atmospheric emission inventory of polycyclic aromatic hydrocarbons (PAHs) for 2004, Atmos. Environ., 43, 812-819, 10.1016/j.atmosenv.2008.10.050, 2009.

Zhulidov, A. V., Robarts, R. D., Pavlov, D. F., Kamari, J., Gurtovaya, T. Y., Merilainen, J. J., and Pospelov, I. N.: Long-term changes of heavy metal and sulphur concentrations in ecosystems of the Taymyr Peninsula (Russian Federation) North of the Norilsk Industrial Complex, Environ. Monit. Assess., 181, 539-553, 10.1007/s10661-010-1848-y, 2011.

Figure caption list

Figure 1. Locations of investigated islands for soil sampling and trajectory of the vessel in the Russian Arctic.

Figure 2. Occurrence of heavy metals. Results show the concentrations of heavy metals in the **(a)** gas phase, **(b)** aerosol phase, **(c)** and dissolved water phase. Colored bars show the sum of nine quantified metals. The number at the bottom of the legend bars represent the concentration scale as same as Figure 3-7.

Figure 3. Measured atmosphere–ocean exchange of heavy metals. **(a)** Fluxes of dry deposition for nine heavy metals; **(b)** fluxes of net diffusive air–water exchange for Hg. In panel **(a)**, colored bars represent the sum of nine heavy metals. In panel **(b)**, downward bars represent the net deposition into the ocean, and upward bars represent the net volatilization of Hg.

Figure 4. Wet deposition of **(a)** heavy metals and **(b)** PAH fluxes. The measured wet deposition of heavy metals and PAHs occurred during the eight snow events encountered during the vessel expedition.

Figure 5. Occurrence of PAHs in the Russian Arctic Ocean. Concentrations of PAHs in the **(a)** gas phase, **(b)** aerosol phase, and **(c)** dissolved water phase. Color bars indicate the sum of 35 PAHs, where each PAH corresponds to the bottom legend (colors range from red for the heaviest molecular weight PAHs to green for the lightest molecular weight PAHs).

Figure 6. Dry deposition fluxes for the 35 measured PAHs. Color bars indicate the sum of the 35 quantified compounds, and each color represents the individual PAHs in the bottom legend (colors range from red for the heaviest molecular weight PAHs to green for the lightest molecular weight PAHs).

Figure 7. Measured atmosphere–ocean exchange of PAHs. **(a)** net diffusive air–water exchange fluxes (all net deposition into the ocean) and **(b)** volatilization air–water exchange fluxes. Color bars indicate the sum of the 35 quantified compounds, and each color represents the individual PAHs in the bottom legend (colors range from red for the heaviest molecular weight PAHs to green for the lightest molecular weight PAHs).

Figure 8. Atmospheric degradation of PAHs. Estimated fluxes of degraded PAHs in the gas phase following reaction with OH radicals.

~~**Figure 6.** Measured atmosphere–ocean exchange of PAHs. **(a)** Dry deposition fluxes for the 35 measured PAHs; **(b)** net diffusive air–water exchange fluxes (all net deposition into the ocean) for fluoranthene, tetramethylphenanthrene, trimethylphenanthrene, and dibenzothiophene. Color bars indicate the sum of the 35 quantified compounds, and each color represents the individual PAHs in the bottom legend (colors range from red for the heaviest molecular weight PAHs to green for the lightest molecular weight PAHs).~~

~~**Figure 7.** Atmospheric degradation of PAHs. Estimated fluxes of degraded PAHs in the gas phase following reaction with OH radicals.~~

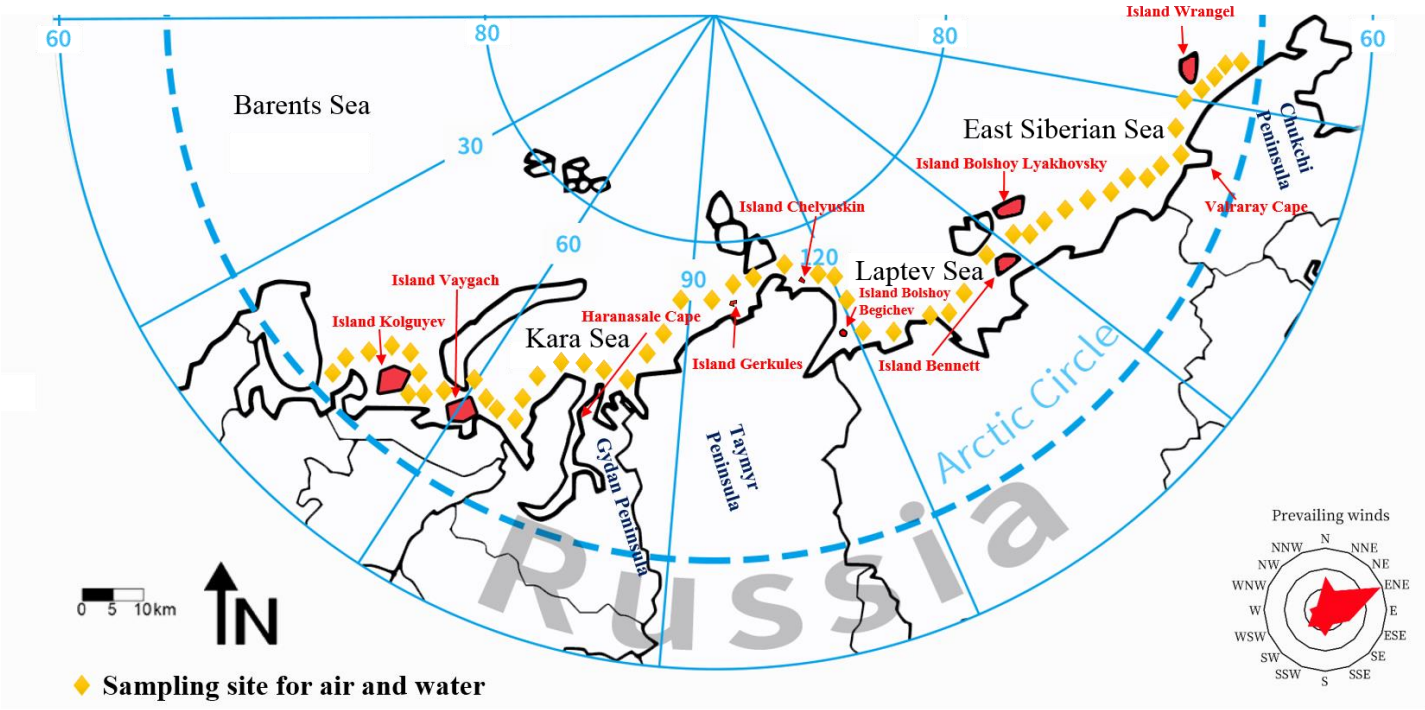
Barents Sea
Kara Sea
Laptev Sea
East Siberian Sea
Russia
Arctic Circle
Island Wrangel
Island Bolshoy Lyakhovsky
Island Chelyuskin
Island Vaygach
Island Kolguyev
Haranasale Cape
Island Gerkules
Island Bolshoy Begichev
Island Bennett
Vaiaray Cape
Chukchi Peninsula
Gydan Peninsula
Taymyr Peninsula
60
80
30
90
120
0 5 10km
N
Prevailing winds
Sampling site for air and water

Figure 1.

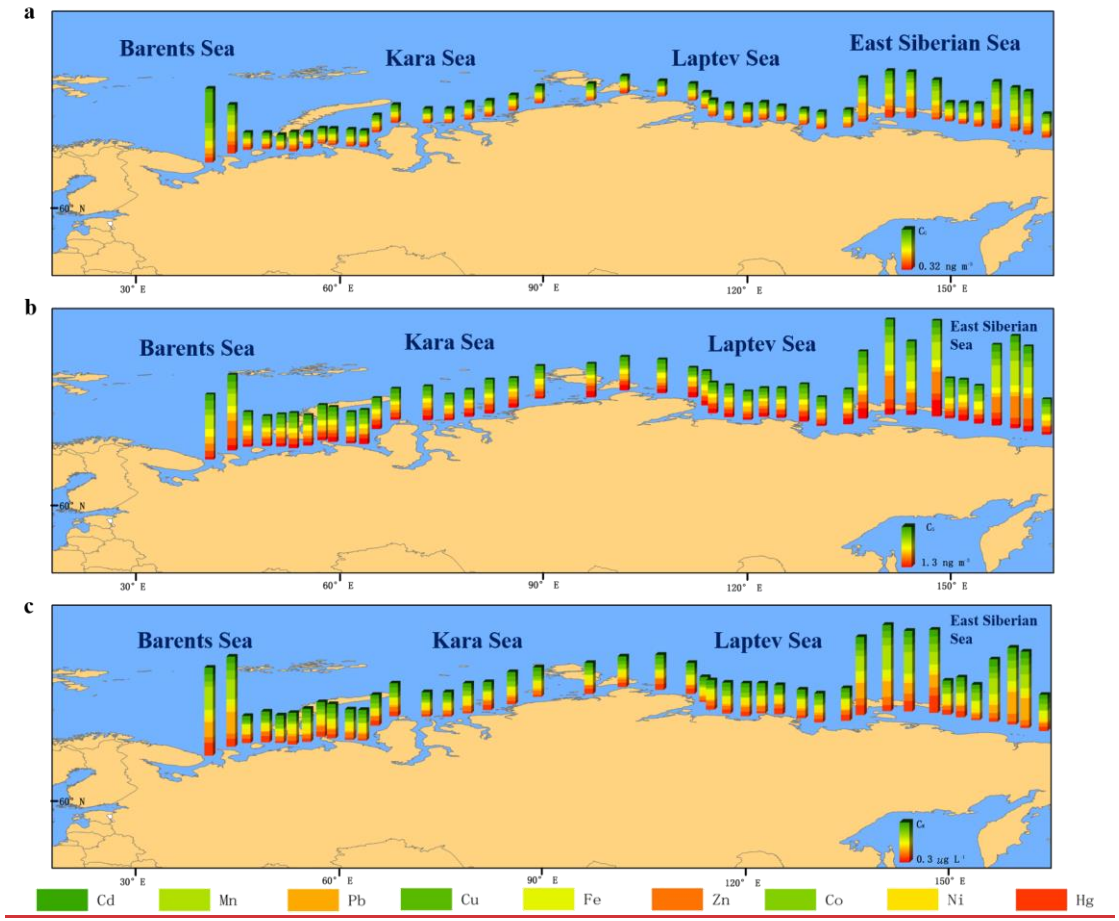

带格式的: 左侧: 2.36 厘米, 右侧: 0.99 厘米, 顶端: 1.65 厘米, 底端: 1.65 厘米, 宽度: 29.7 厘米, 高度: 21 厘米, 指定行网格

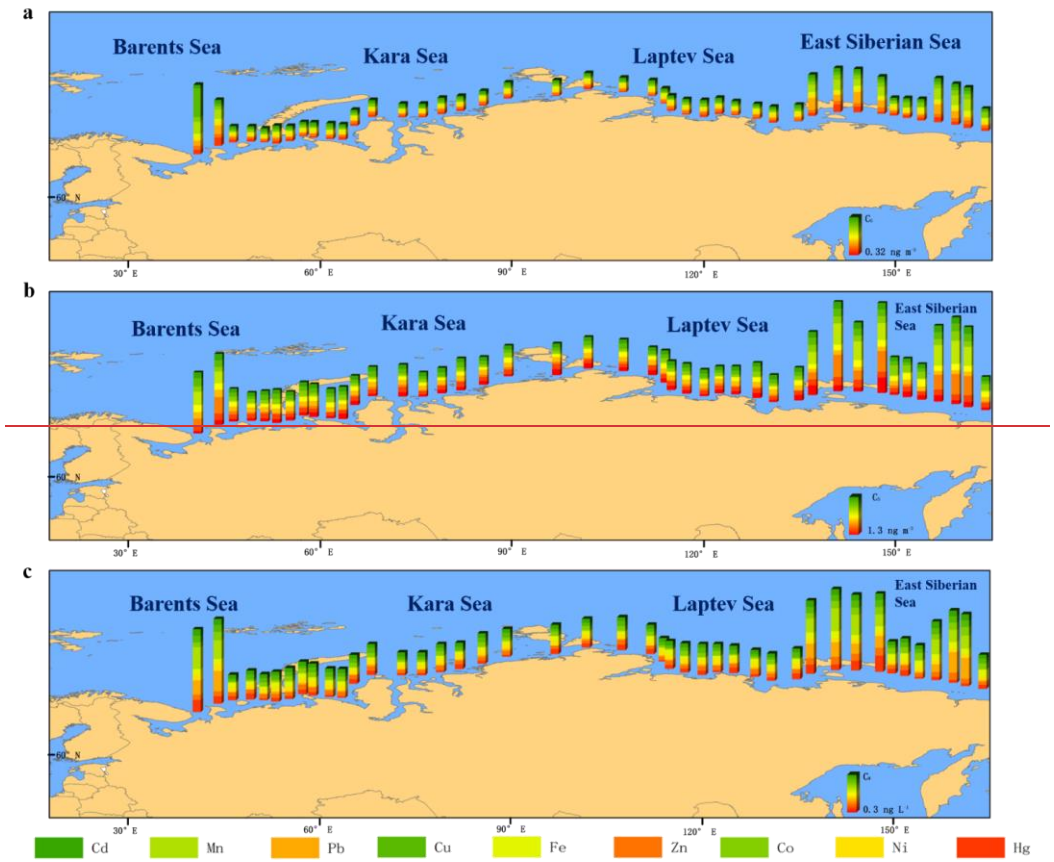
a
Barents Sea
Kara Sea
Laptev Sea
East Siberian Sea
60° N
30° E
60° E
90° E
120° E
150° E
0.32 ng m⁻³
b
Barents Sea
Kara Sea
Laptev Sea
East Siberian Sea
1.3 ng m⁻³
c
Barents Sea
Kara Sea
Laptev Sea
East Siberian Sea
0.3 ng L⁻¹
Cd
Mn
Pb
Cu
Fe
Zn
Co
Ni
Hg

Figure 2.

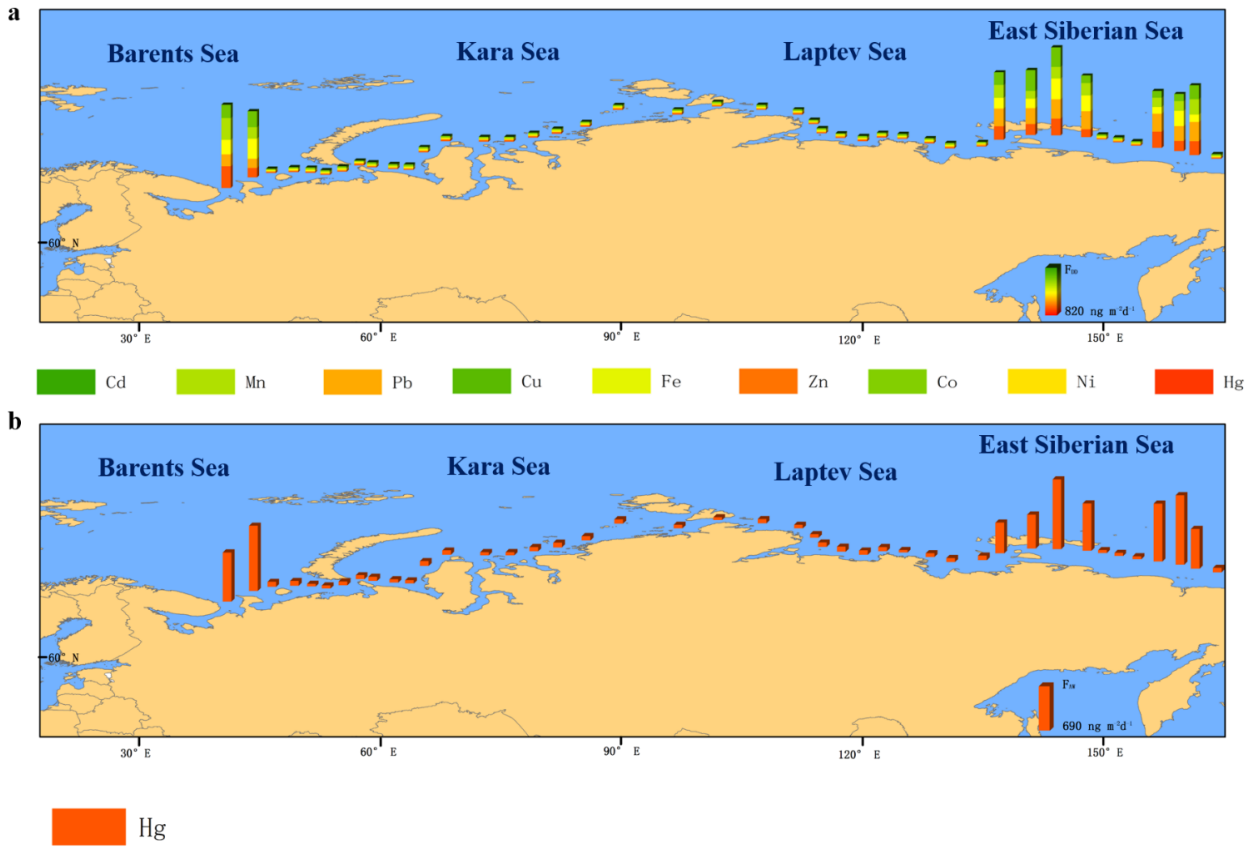
a
Barents Sea
Kara Sea
Laptev Sea
East Siberian Sea
60° N
820 ng m⁻²d⁻¹
30° E
60° E
90° E
120° E
150° E
Cd
Mn
Pb
Cu
Fe
Zn
Co
Ni
Hg
b
Barents Sea
Kara Sea
Laptev Sea
East Siberian Sea
60° N
690 ng m⁻²d⁻¹
30° E
60° E
90° E
120° E
150° E
Hg

Figure 3.

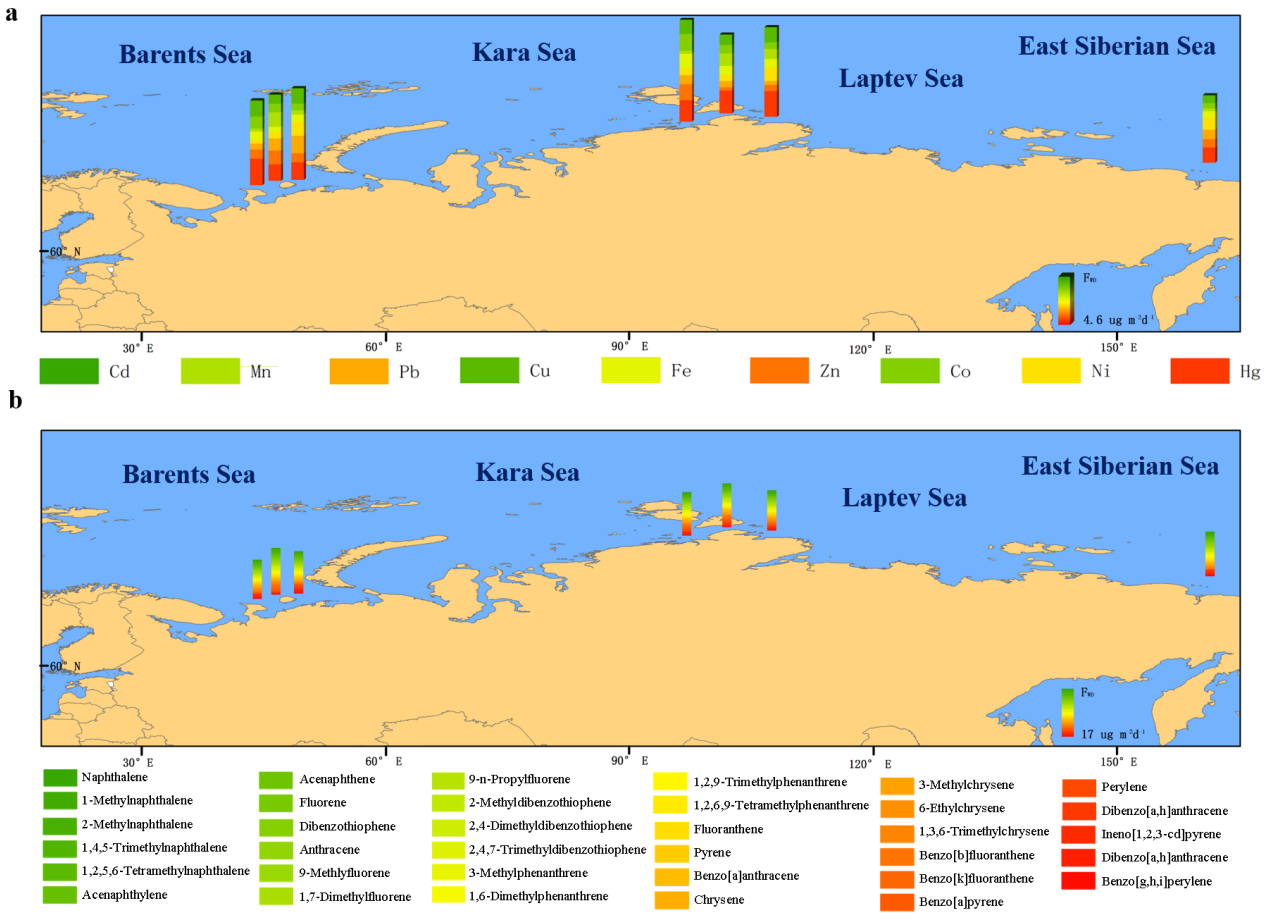
a
Barents Sea
Kara Sea
Laptev Sea
East Siberian Sea
60° N
30° E
60° E
90° E
120° E
150° E
4.6 ug m⁻²d⁻¹
Cd
Mn
Pb
Cu
Fe
Zn
Co
Ni
Hg
b
Barents Sea
Kara Sea
Laptev Sea
East Siberian Sea
60° N
30° E
60° E
90° E
120° E
150° E
17 ug m⁻²d⁻¹
Naphthalene
1-Methylnaphthalene
2-Methylnaphthalene
1,4,5-Trimethylnaphthalene
1,2,5,6-Tetramethylnaphthalene
Acenaphthylene
Acenaphthene
Fluorene
Dibenzothiophene
Anthracene
9-Methlyfluorene
1,7-Dimethylfluorene
9-n-Propylfluorene
2-Methyldibenzothiophene
2,4-Dimethyldibenzothiophene
2,4,7-Trimethyldibenzothiophene
3-Methylphenanthrene
1,6-Dimethylphenanthrene
1,2,9-Trimethylphenanthrene
1,2,6,9-Tetramethylphenanthrene
Fluoranthene
Pyrene
Benzo[a]anthracene
Chrysene
3-Methylchrysene
6-Ethylchrysene
1,3,6-Trimethylchrysene
Benzo[b]fluoranthene
Benzo[k]fluoranthene
Benzo[a]pyrene
Perylene
Dibenzo[a,h]anthracene
Ineno[1,2,3-cd]pyrene
Dibenzo[a,h]anthracene
Benzo[g,h,i]perylene

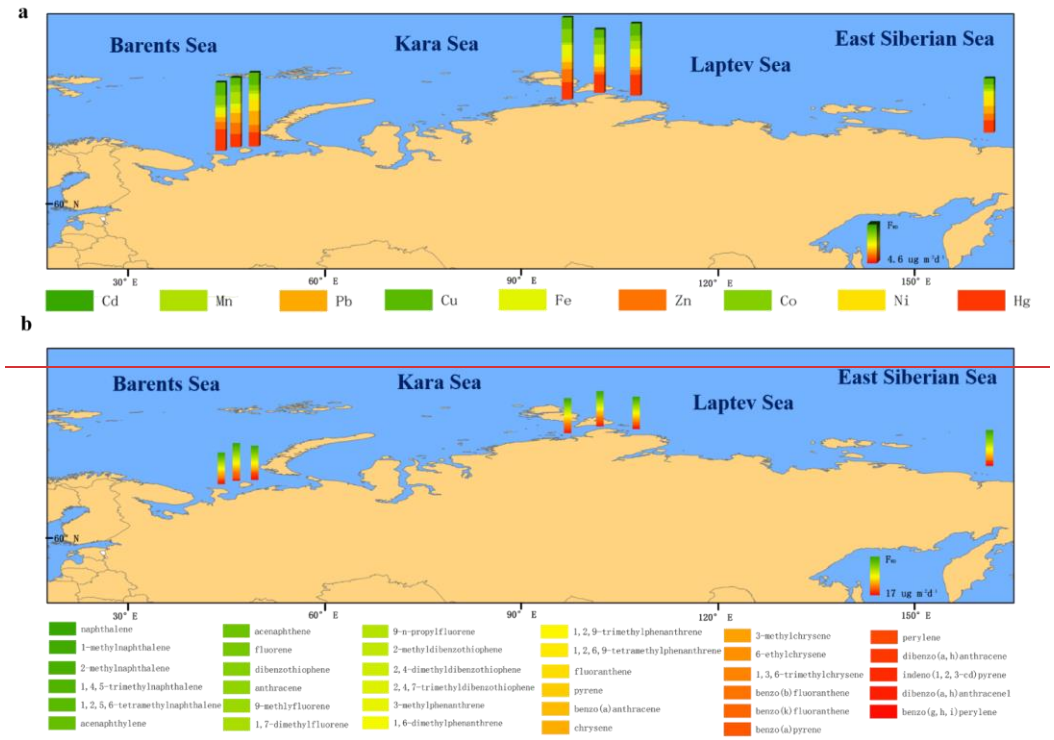
a
Barents Sea
Kara Sea
Laptev Sea
East Siberian Sea
60° N
30° E
60° E
90° E
120° E
150° E
4.6 ug m-2 d-1
Cd
Mn
Pb
Cu
Fe
Zn
Co
Ni
Hg
b
Barents Sea
Kara Sea
Laptev Sea
East Siberian Sea
60° N
30° E
60° E
90° E
120° E
150° E
17 ug m-2 d-1
naphthalene
1-methylnaphthalene
2-methylnaphthalene
1, 4, 5-trimethylnaphthalene
1, 2, 5, 6-tetramethylnaphthalene
acenaphthylene
acenaphthene
fluorene
dibenzothiophene
anthracene
9-methlyfluorene
1, 7-dimethylfluorene
9-n-propylfluorene
2-methyldibenzothiophene
2, 4-dimethyldibenzothiophene
2, 4, 7-trimethyldibenzothiophene
3-methylphenanthrene
1, 6-dimethylphenanthrene
1, 2, 9-trimethylphenanthrene
1, 2, 6, 9-tetramethylphenanthrene
fluoranthene
pyrene
benzo(a)anthracene
chrysene
3-methylchrysene
6-ethylchrysene
1, 3, 6-trimethylchrysene
benzo(b)fluoranthene
benzo(k)fluoranthene
benzo(a)pyrene
perylene
dibenzo(a, h)anthracene
indeno(1, 2, 3-cd)pyrene
dibenzo(a, h)anthracene1
benzo(g, h, i)perylene

Figure 4.

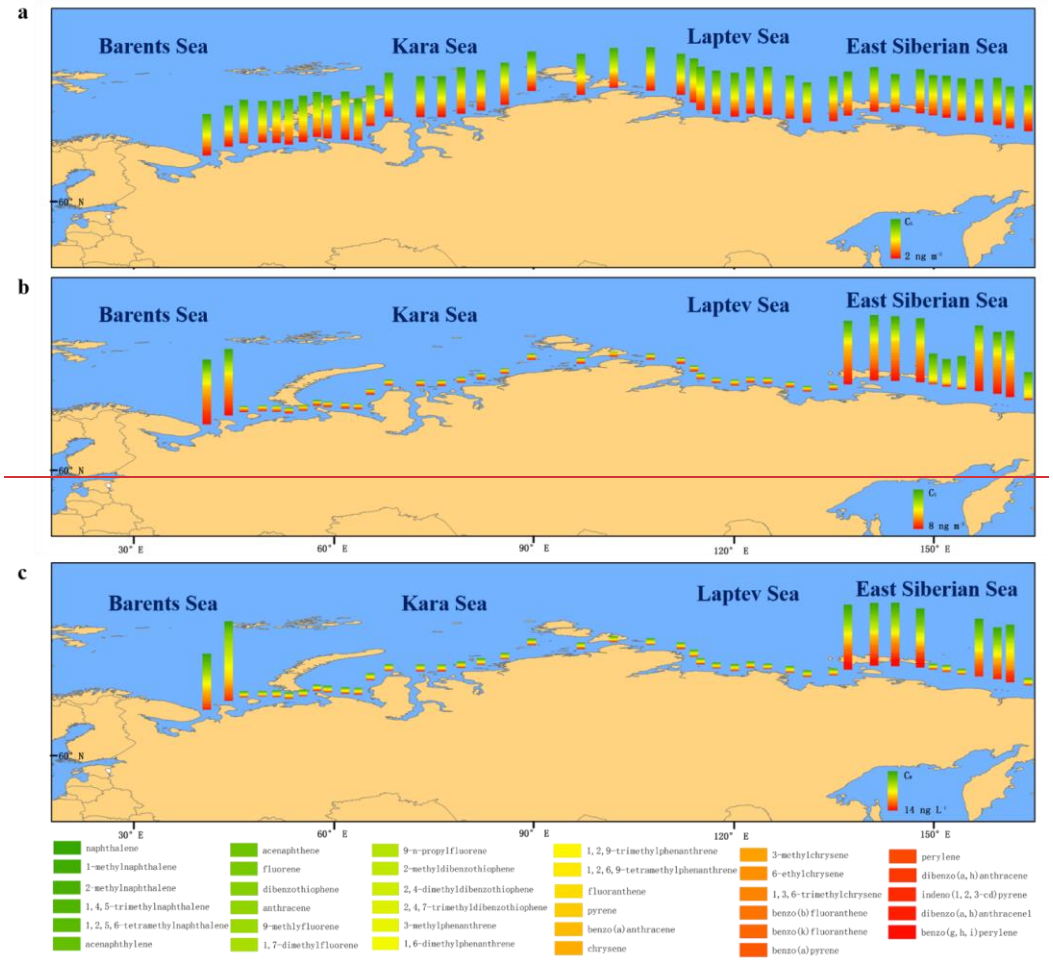
a
Barents Sea
Kara Sea
Laptev Sea
East Siberian Sea
60° N
Cv
2 ng m⁻³
b
Barents Sea
Kara Sea
Laptev Sea
East Siberian Sea
60° N
Cv
8 ng m⁻³
30° E
60° E
90° E
120° E
150° E
c
Barents Sea
Kara Sea
Laptev Sea
East Siberian Sea
60° N
Cv
14 ng L⁻¹
30° E
60° E
90° E
120° E
150° E
naphthalene
1-methylnaphthalene
2-methylnaphthalene
1, 4, 5-trimethylnaphthalene
1, 2, 5, 6-tetramethylnaphthalene
acenaphthylene
acenaphthene
fluorene
dibenzothiophene
anthracene
9-methylfluorene
1, 7-dimethylfluorene
9-n-propylfluorene
2-methyldibenzothiophene
2, 4-dimethyldibenzothiophene
2, 4, 7-trimethyldibenzothiophene
3-methylphenanthrene
1, 6-dimethylphenanthrene
1, 2, 9-trimethylphenanthrene
1, 2, 6, 9-tetramethylphenanthrene
fluoranthene
pyrene
benzo(a)anthracene
chrysene
3-methylchrysene
6-ethylchrysene
1, 3, 6-trimethylchrysene
benzo(b)fluoranthene
benzo(k)fluoranthene
benzo(a)pyrene
perylene
dibenzo(a, h)anthracene
indeno(1, 2, 3-cd)pyrene
dibenzo(a, h)anthracene1
benzo(g, h, i)perylene

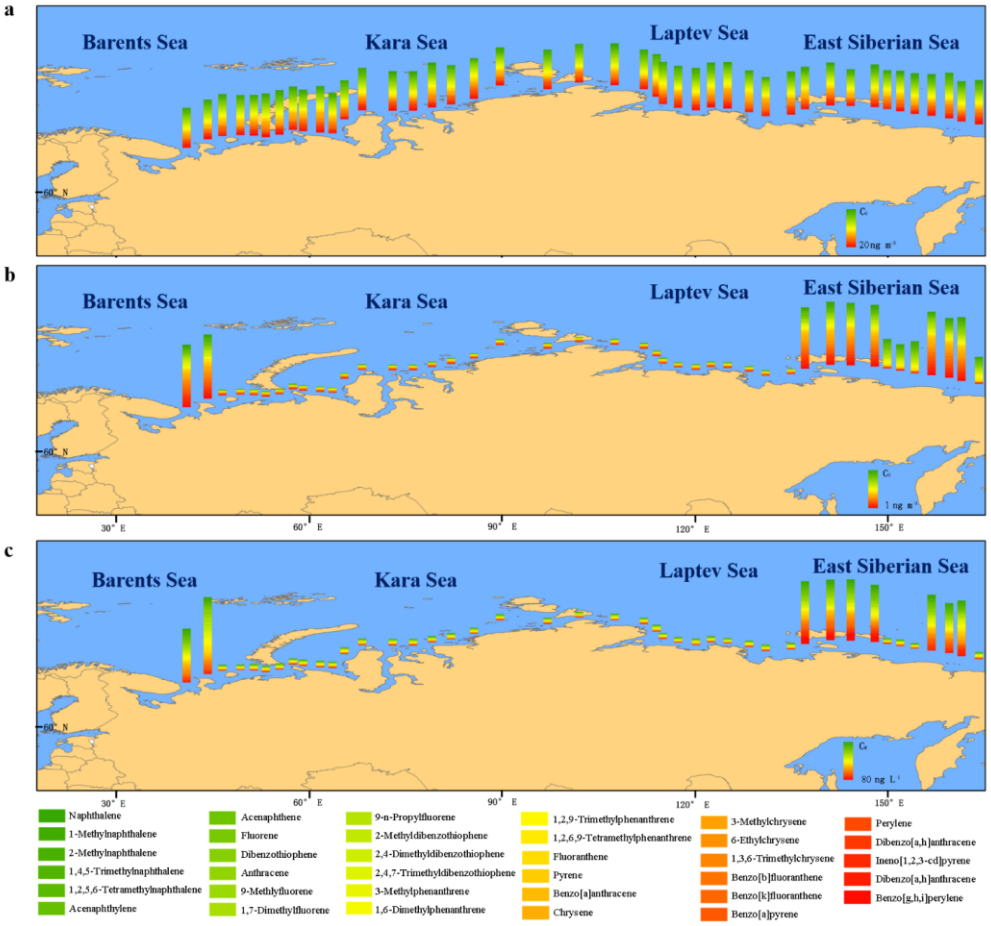
a
Barents Sea
Kara Sea
Laptev Sea
East Siberian Sea
60° N
Cs
20 ng m⁻³
b
Barents Sea
Kara Sea
Laptev Sea
East Siberian Sea
60° N
Cs
1 ng m⁻³
30° E
60° E
90° E
120° E
150° E
c
Barents Sea
Kara Sea
Laptev Sea
East Siberian Sea
60° N
Cs
80 ng L⁻¹
30° E
60° E
90° E
120° E
150° E
Naphthalene
1-Methylnaphthalene
2-Methylnaphthalene
1,4,5-Trimethylnaphthalene
1,2,5,6-Tetramethylnaphthalene
Acenaphthylene
Acenaphthene
Fluorene
Dibenzothiophene
Anthracene
9-Methylfluorene
1,7-Dimethylfluorene
9-n-Propylfluorene
2-Methyldibenzothiophene
2,4-Dimethyldibenzothiophene
2,4,7-Trimethyldibenzothiophene
3-Methylphenanthrene
1,6-Dimethylphenanthrene
1,2,9-Trimethylphenanthrene
1,2,6,9-Tetramethylphenanthrene
Fluoranthene
Pyrene
Benzo[a]anthracene
Chrysene
3-Methylchrysene
6-Ethylchrysene
1,3,6-Trimethylchrysene
Benzo[b]fluoranthene
Benzo[k]fluoranthene
Benzo[a]pyrene
Perylene
Dibenzo[a,h]anthracene
Ineno[1,2,3-cd]pyrene
Dibenzo[a,h]anthracene
Benzo[g,h,i]perylene

Figure 5.

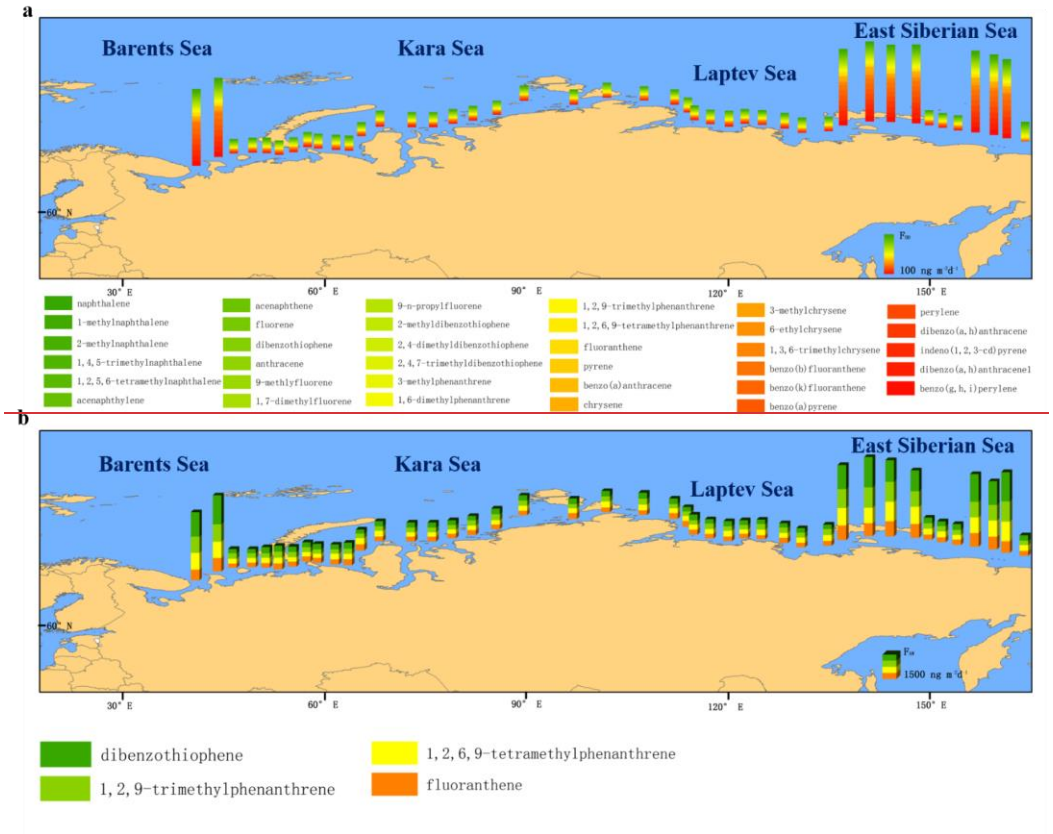
a
Barents Sea
Kara Sea
Laptev Sea
East Siberian Sea
60° N
30° E
60° E
90° E
120° E
150° E
Fw
100 ng m-2d-1
naphthalene
1-methylnaphthalene
2-methylnaphthalene
1, 4, 5-trimethylnaphthalene
1, 2, 5, 6-tetramethylnaphthalene
acenaphthylene
acenaphthene
fluorene
dibenzothiophene
anthracene
9-methylfluorene
1, 7-dimethylfluorene
9-n-propylfluorene
2-methyldibenzothiophene
2, 4-dimethyldibenzothiophene
2, 4, 7-trimethyldibenzothiophene
3-methylphenanthrene
1, 6-dimethylphenanthrene
1, 2, 9-trimethylphenanthrene
1, 2, 6, 9-tetramethylphenanthrene
fluoranthene
pyrene
benzo(a)anthracene
chrysene
3-methylchrysene
6-ethylchrysene
1, 3, 6-trimethylchrysene
benzo(b)fluoranthene
benzo(k)fluoranthene
benzo(a)pyrene
perylene
dibenzo(a, h)anthracene
indeno(1, 2, 3-cd)pyrene
dibenzo(a, h)anthracene1
benzo(g, h, i)perylene
b
Barents Sea
Kara Sea
Laptev Sea
East Siberian Sea
60° N
30° E
60° E
90° E
120° E
150° E
Fw
1500 ng m-2d-1
dibenzothiophene
1, 2, 9-trimethylphenanthrene
1, 2, 6, 9-tetramethylphenanthrene
fluoranthene

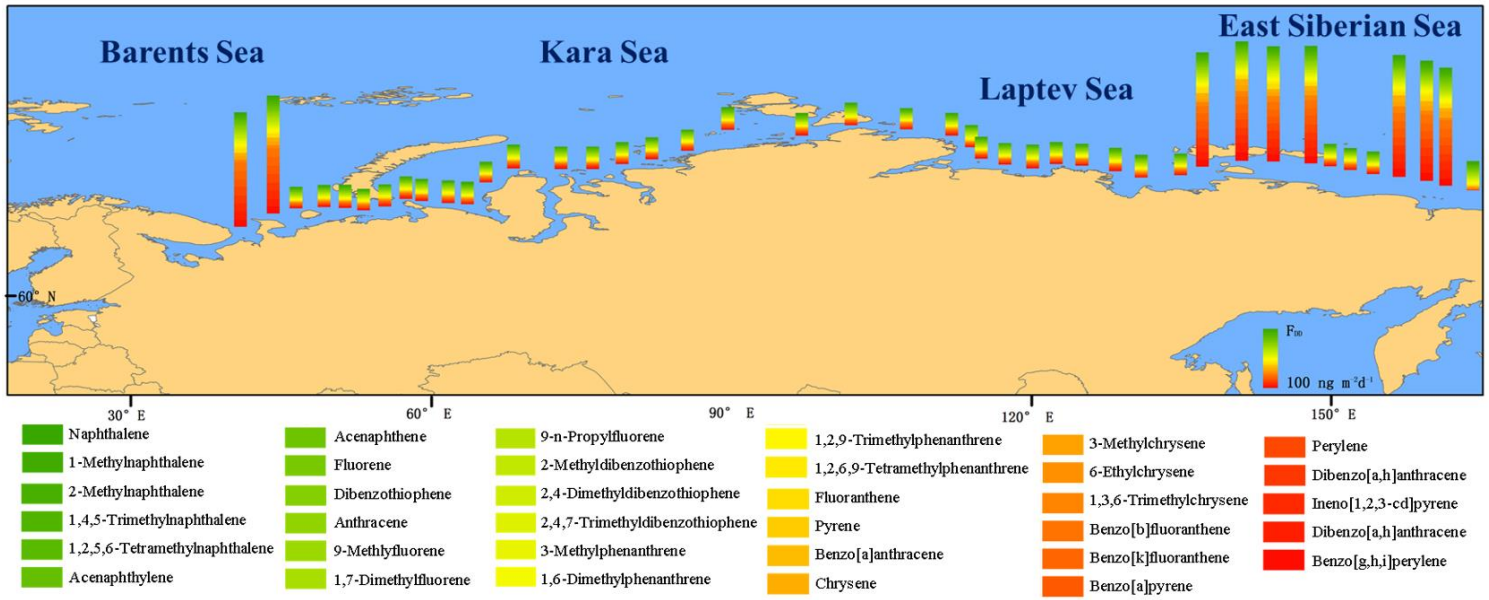
Barents Sea
Kara Sea
Laptev Sea
East Siberian Sea
60° N
30° E
60° E
90° E
120° E
150° E
Fm
100 ng m-2d-1
Naphthalene
1-Methylnaphthalene
2-Methylnaphthalene
1,4,5-Trimethylnaphthalene
1,2,5,6-Tetramethylnaphthalene
Acenaphthylene
Acenaphthene
Fluorene
Dibenzothiophene
Anthracene
9-Methlyfluorene
1,7-Dimethylfluorene
9-n-Propylfluorene
2-Methyldibenzothiophene
2,4-Dimethyldibenzothiophene
2,4,7-Trimethyldibenzothiophene
3-Methylphenanthrene
1,6-Dimethylphenanthrene
1,2,9-Trimethylphenanthrene
1,2,6,9-Tetramethylphenanthrene
Fluoranthene
Pyrene
Benzo[a]anthracene
Chrysene
3-Methylchrysene
6-Ethylchrysene
1,3,6-Trimethylchrysene
Benzo[b]fluoranthene
Benzo[k]fluoranthene
Benzo[a]pyrene
Perylene
Dibenzo[a,h]anthracene
Ineno[1,2,3-cd]pyrene
Dibenzo[a,h]anthracene
Benzo[g,h,i]perylene

Figure 6.

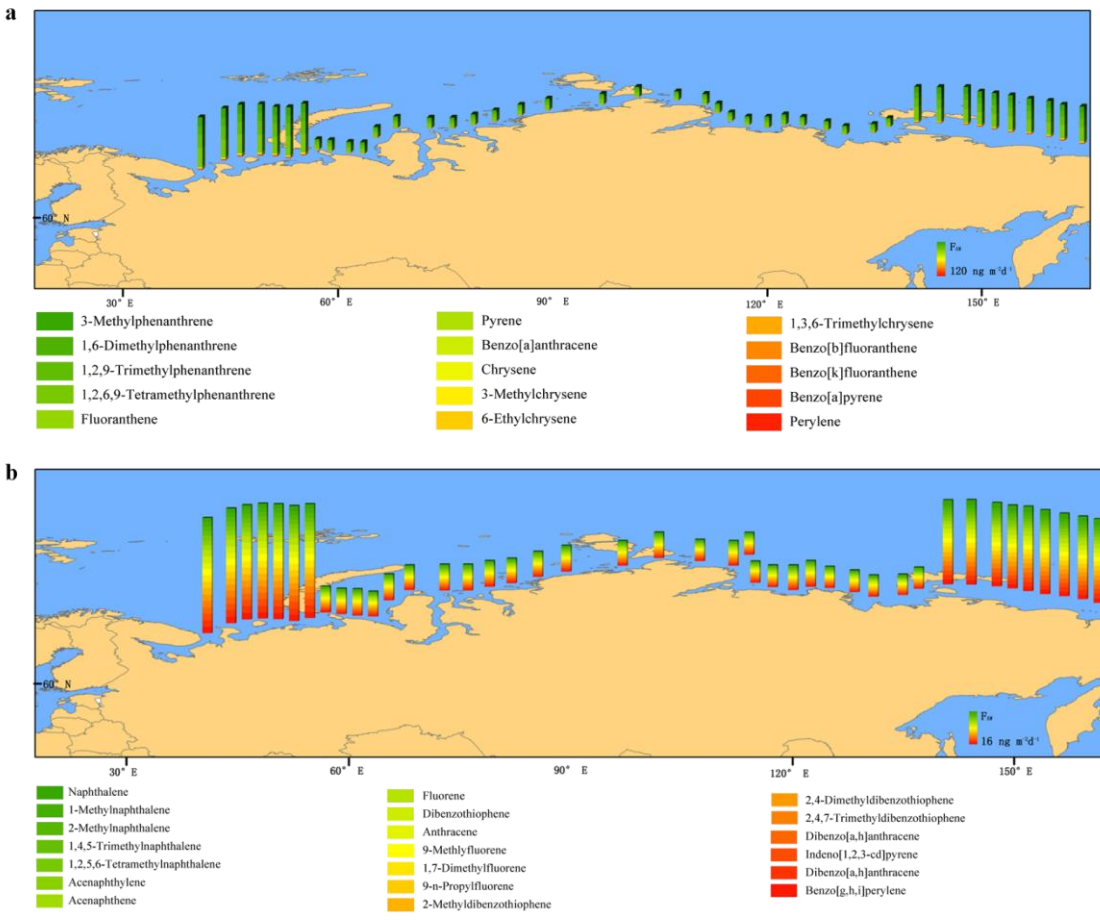
a
60° N
30° E
60° E
90° E
120° E
150° E
120 ng m⁻²d⁻¹
3-Methylphenanthrene
1,6-Dimethylphenanthrene
1,2,9-Trimethylphenanthrene
1,2,6,9-Tetramethylphenanthrene
Fluoranthene
Pyrene
Benzo[a]anthracene
Chrysene
3-Methylchrysene
6-Ethylchrysene
1,3,6-Trimethylchrysene
Benzo[b]fluoranthene
Benzo[k]fluoranthene
Benzo[a]pyrene
Perylene
b
60° N
30° E
60° E
90° E
120° E
150° E
16 ng m⁻²d⁻¹
Naphthalene
1-Methylnaphthalene
2-Methylnaphthalene
1,4,5-Trimethylnaphthalene
1,2,5,6-Tetramethylnaphthalene
Acenaphthylene
Acenaphthene
Fluorene
Dibenzothiophene
Anthracene
9-Methylfluorene
1,7-Dimethylfluorene
9-n-Propylfluorene
2-Methyldibenzothiophene
2,4-Dimethyldibenzothiophene
2,4,7-Trimethyldibenzothiophene
Dibenzo[a,h]anthracene
Indeno[1,2,3-cd]pyrene
Dibenzo[a,h]anthracene
Benzo[g,h,i]perylene

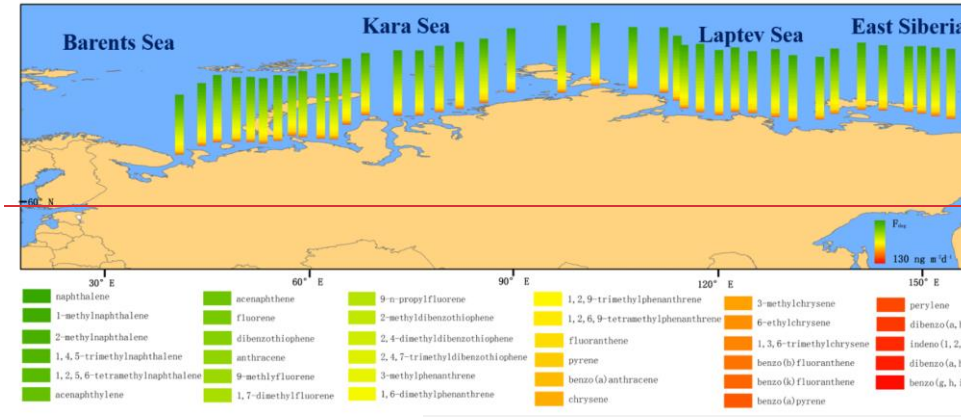
Barents Sea
Kara Sea
Laptev Sea
East Siberia
60° N
30° E
60° E
90° E
120° E
150° E
130 ng m⁻²d⁻¹
naphthalene
1-methylnaphthalene
2-methylnaphthalene
1, 4, 5-trimethylnaphthalene
1, 2, 5, 6-tetramethylnaphthalene
acenaphthylene
acenaphthene
fluorene
dibenzothiophene
anthracene
9-methlyfluorene
1, 7-dimethylfluorene
9-n-propylfluorene
2-methyldibenzothiophene
2, 4-dimethyldibenzothiophene
2, 4, 7-trimethyldibenzothiophene
3-methylphenanthrene
1, 6-dimethylphenanthrene
1, 2, 9-trimethylphenanthrene
1, 2, 6, 9-tetramethylphenanthrene
fluoranthene
pyrene
benzo(a)anthracene
chrysene
3-methylchrysene
6-ethylchrysene
1, 3, 6-trimethylchrysene
benzo(b)fluoranthene
benzo(k)fluoranthene
benzo(a)pyrene
perylene

Figure 7.

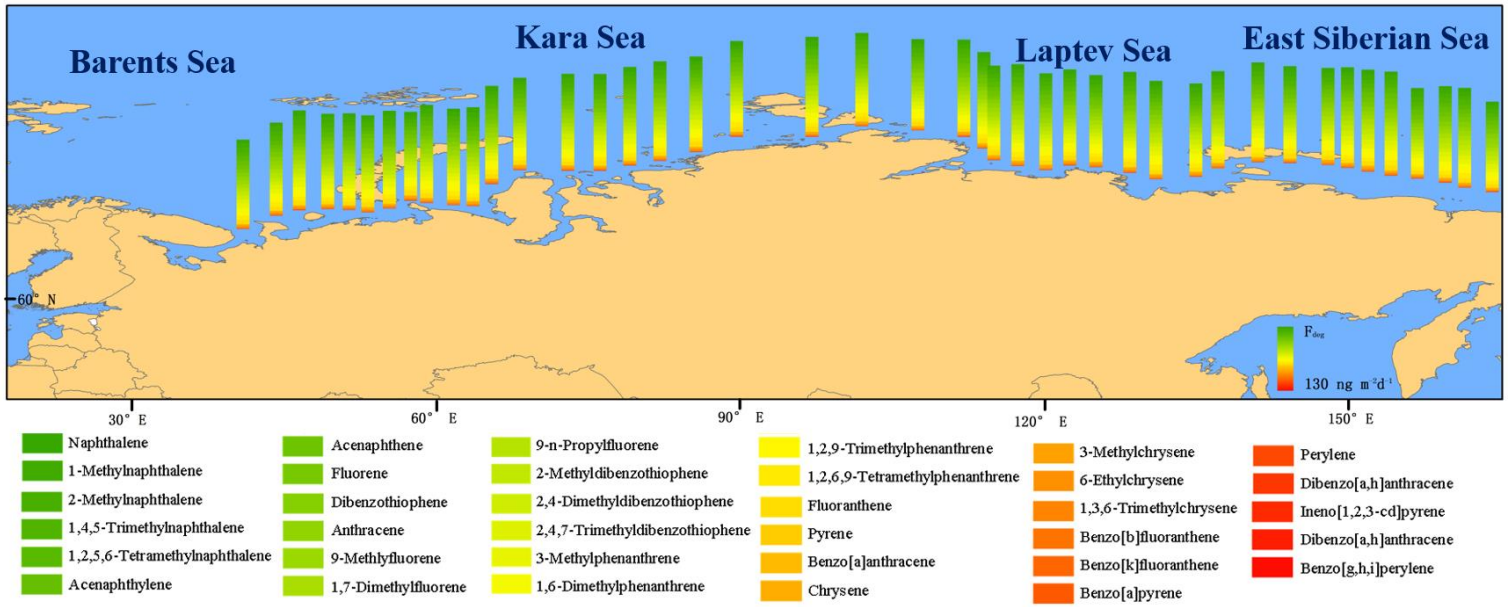

Figure 8.